

THE STATIC AND DYNAMIC PERFORMANCE
CHARACTERISTICS OF THE KSU SAVONIUS WIND ROTOR

by

SHAILESH HARIPRASAD PATEL

B.E., The Maharaja Sayajirao University Of Baroda, India, 1973

A MASTER'S THESIS

submitted in partial fulfillment of the
requirements for the degree

MASTER OF SCIENCE


Department of Mechanical Engineering

Kansas State University

Manhattan, Kansas

1977

Approved By:



Major Professor

LD
2668
T4
1977
P38
C.2

407

Document TABLE OF CONTENTS

Chapter	Page
NOMENCLATURE	v
I. INTRODUCTION.....	1
II. WIND-ELECTRIC POWER GENERATING SYSTEM.....	5
Wind Rotor	5
Belt Power Transmission	5
Alternator	7
III. EXPERIMENTAL TESTING.....	8
Test Set-up	8
Test Procedure	10
IV. REDUCTION AND ANALYSIS OF DATA.....	12
V. MATHEMATICAL MODELLING.....	19
Static Characteristics	19
Wind Rotor-Alternator System Dynamics	24
VI. ANALYSIS OF THE STATIC PERFORMANCE CHARACTERISTICS.....	28
Loci Of Constant Load On C_p vs. TSR Characteristic	28
Case I: Operation At Constant Load	29
Case II: Operation At Maximum Coefficient Of Power	32
Case III: Operation At Constant Speed	32
VII. TIME-DOMAIN ANALYSIS.....	40
Transient Response	40
Transfer Function	44
VIII. CONCLUSIONS AND RECOMMENDATIONS.....	47
IX. LIST OF REFERENCES.....	49
APPENDIX I.....	51
APPENDIX II.....	53
APPENDIX III.....	56

LIST OF FIGURES

Figure	Page
1. KSU Wind Rotor	6
2. Block Diagram Of Instrumentation For Measurement Of Variables	9
3. Calculated Results For A Typical "Steady State" Interval	15
4. Actual Data And Curve For Coefficient Of Power versus Tip Speed Ratio	16
5. Coefficient Of Power versus Tip Speed Ratio	17
6. Wind Rotor Torque - Speed Characteristics	23
7. Schematic Of Wind-Electrical Power Generating System	25
8. Loci Of Constant Load On C_p versus TSR Characteristics	30
9. Load Resistance versus Wind Speed For Maximum C_p Operation	33
10. Closed Loop System To Regulate The Load Resistance For Maximum C_p Operation	34
11. Loci Of Constant Load Resistance On Torque-Rotor Speed Characteristic	36
12. Desired Load Resistance versus Wind Speed For Constant Rotor Speed Operation	38
13. Closed Loop System To Regulate The Load Resistance For Constant Rotor Speed Operation	39
14. Transient Response Of Rotor For $R_L = 0.657$ ohms	42
15. Transient Response Of Rotor For $R_L = 1.333$ ohms	44
16. Wind Rotor Gain Constant versus Load Resistance	46

LIST OF TABLES

Table		Page
1	Load Resistance For Maximum Coefficient Of Power Operation.....	31
2	Wind Rotor Performance At A Constant Speed.....	37

NOMENCLATURE

B_{eq}	Equivalent Damping Of The Rotating Parts Referred To Rotor Shaft	ft.lbf.sec/rad
B_r	Damping Of Wind Rotor	ft.lbf.sec/rad
B_a	Damping Of Alternator Rotating Parts	ft.lbf.sec/rad
C_p	Coefficient Of Power	dimensionless
D_a	Diameter Of Driving Pulley	feet
D_r	Diameter Of Driven Pulley	feet
E_b	Back EMF Of Alternator	volts
I_L	Load Current	amperes
J_{eq}	Equivalent Inertia Of The Rotating Parts Referred To Rotor Shaft	ft.lbf.sec ²
J_r	Inertia Of Wind Rotor	ft.lbf.sec ²
J_a	Inertia Of Alternator Rotor	ft.lbf.sec ²
L_a	Inductance Of Armature Circuit	henrys
N_a	Alternator Rotor Revolutions	RPM
N_r	Wind Rotor Revolutions	RPM
L_f	Inductance Of Field Winding	henrys
$N_r(s)$	Laplace Transform Of Wind Rotor Revolutions	
$N_r(0)$	Laplace Transform Of Rotor RPM(initial)	
P_{elect}	Electrical Power Loss In Alternator	watts
P_{fw}	Friction and Windage Loss In Alternator	watts
P_{out}	Power Output At The Load Terminals	watts
P_{mech}	Mechanical Power Developed At Rotor Shaft	watts
P_{wind}	Theoretical Power In The Wind	watts

R_a	Alternator Armature Circuit Resistance	watts
R_L	Load Resistance	ohms
R_f	Field Circuit Resistance	ohms
S	Laplace Operator	1/seconds
t	Time	seconds
T_{dev}	Torque Developed By Wind Rotor	ft.lbf.
T_{ref}	Torque Reflected To The Wind Rotor Shaft	ft.lbf.
T_a	Electrical Time Constant	seconds
T_r	Rotor Time Constant	seconds
TSR	Tip Speed Ratio	dimensionless
U	Tip Velocity Of The Wind Rotor	ft./sec
V_f	Field Voltage	volts
V_w	Wind Speed	MPH
$V_w(s)$	Laplace Transform Of Change In Wind Speed	
V_L	Load Voltage	volts
V_{oc}	Open Circuit Voltage	volts
T_m	Time Constant Of Actuator	seconds
K_m	Gain Constant Of Servo Type Actuator	
ϵ	Error Signal	
ω_r	Angular Velocity Of Rotor	radian/sec.
K_r	Wind Rotor Gain Constant	RPM/MPH
A	projected area of wind rotor(57.5 ft ²)	sq. ft.

CHAPTER I

INTRODUCTION

Historically, wind power has been used for centuries for sailing vessels and as a source of power in the northern parts of Europe. In Holland, large wind mills have been used for pumping water in reclaiming land. The Dutch, not blessed with large fossil energy resources, harnessed what they had, the wind blowing in from the North sea. In America, the plains area of the midwest are marked with multibladed windmills that have been used for pumping water for more than fifty years. In midwest area, the wind power has also been used for generating electricity as evidenced abandoned wind-electric plants which utilized the propeller type of wind rotor.

The biggest generator built to date was the Smith-Putnam wind rotor that operated atop Grandpa's knob, Vermont, from 1941 to 1945. It developed 1250 Kw at 29 RPM in a 24 MPH breeze. The project was abandoned when one of the 8-ton blades failed mechanically. During the 1930's and 1940's, when America began to emerge as a leading industrial giant and world power, the need for energy skyrocketed and new sources had to be found. Because the power supplied by REA(Rural Electrification Administration) was so cheap, interest in and further development of wind power came to a halt.

The applications presently under consideration are pumping water out of wells, generation of electricity for grid supply, storing the charge in the batteries to generate hydrogen from the water later on by

electrolysis. The hydrogen would then be used as a fuel in engines.

Except for a rather inventive period in the 1920's, the approach taken to extracting power from the wind has been that of using blades or vanes rotating about a horizontal axis. In 1929, after several years of work, S.J. Savonius, a Finish engineer, patented a vertical axis, or S-type, wind rotor and in 1931 G.J.M. Darrieus also patented a vertical axis wind rotor.

Savonius(10) started his work in 1924 and did experiments on fifty different models in a wind tunnel. Of these fifty models more than thirty were vertical axis S-type rotors with varying vane form, size of central air passage and aspect ratio. Aspect ratio is obtained by dividing height of the rotor by diameter. The best of the S-rotors gave a thirty percent coefficient of power (efficiency). After completion of wind tunnel tests Savonius continued his testing in the natural wind, and obtained higher coefficient of power than in the wind tunnel. Values as high as thirty seven percent in natural wind were claimed by Savonius.

In 1974 Carver and McPherson(2) investigated the possibility of using Savonius type rotors for generation of electric power. Their results were quite encouraging. From wind tunnel tests, they concluded that coefficient of power as high as thirty to thirty seven percent could be obtained. Furthermore, they determined that power output varied only slightly over a comparatively wide range of tip speed ratio for a given wind speed. They also observed that the Savonius rotor has a high starting torque which is a very desirable feature.

In 1962 Cretzler, Gaul and Snodgrass(3) reported that the S-rotor is a high inertia rotor, and that acceleration response can be several times faster than deceleration response.

In 1974 Newman(9) did some wind tunnel testing of S-rotors with varying central gap size for a constant Reynold's number and then he tried rotors with

desirable central gaps for different Reynold's numbers and thereby showed the effect of central gap and Reynold's number on the performance of S-rotors.

In 1972 McPherson(7) did a feasibility study to investigate the S-rotor's possible application for powering sailing vessels. From his study he concluded that S-rotors can operate at about thirty percent and higher coefficients of power in winds of as little as 14.32 MPH.

Kentfield(5), in 1974, modified the conventional S-rotor by putting slots in the leading edges, flaps in the trailing edges and other flow guiding surfaces. He compared the conventional S-rotor with modified one and his wind tunnel results indicated coefficients of power as high as fifty five percent for the conventional rotor at a tip speed ratio of about 0.85, and forty three percent for the modified one at a tip speed ratio of 0.5.

Bodek and Simonds(1), in 1964, field tested a Savonius type rotor with a projected area of eighteen square feet. their results showed that the maximum coefficient of power for this rotor was fourteen percent at a tip speed ratio of 0.7. They also considered its application for pumping water out of wells using a diaphragm pump, and concluded that it was best suited for wells less than twenty feet deep.

This thesis is concerned with a Savonius type vertical axis wind rotor, ten feet high and 5.75 feet diameter, which was designed and built at Kansas State University and then field tested during the Summer of 1975. This activity was a joint effort of several faculty and students from the Mechanical and Electrical Engineering departments at K-State. As already mentioned the Savonius type rotor has been experimentally investigated by numerous researchers who have studied effects of geometry on performance, mainly using wind tunnel models.

However, performance characteristics in natural wind for a Savonius

rotor as large as the KSU machine have not been published. Therefore, the first objective of this thesis was to utilize the experimental data obtained from the KSU machine to mathematically model the steady state performance characteristics of the KSU Savonius rotor. The second objective was to develop a computer simulation model for the wind rotor-alternator system in order that its open loop dynamic response could be studied. And the third objective was to investigate the need for a feedback control system in order to obtain maximum system performance.

CHAPTER II

WIND-ELECTRIC POWER GENERATING SYSTEM

The electric power generating system built and tested at KSU is shown in Figure 1. It consisted of a Savonius type wind rotor, belt power transmission drive and an alternator.

A. WIND ROTOR

The Savonius type wind rotor had curved vanes attached to end plates as shown in Figure 1. The rotor diameter was 5.75 feet and the height ten feet giving a projected surface area of 57.5 square feet. The vanes of the rotor were fabricated from fourteen gauge sheet steel, the lower support plate from eleven gauge sheet steel and the upper end plate from sixteen gauge sheet steel. The lower shaft for the rotor, $2\frac{7}{16}$ inches in diameter, was supported by two ball bearings mounted to a steel frame work made of two inch by two inch by $\frac{1}{8}$ inch box tubing located at the bottom of the rotor. A stub shaft, $1\frac{3}{4}$ inches in diameter, at the top of the rotor was supported by a bearing attached to a cable guy wire system. The purpose of this bearing was to prevent vibration.

B. BELT POWER TRANSMISSION DRIVE

The mechanical power from the wind rotor shaft was transmitted to the alternator shaft by a belt and pulley system. The rim attached to the lower support plate of the rotor was used as a driver pulley for the driven pulley mounted on the alternator shaft. The speed ratio was approximately 16:1. Although the angle of contact between the belt and the driven pulley on the

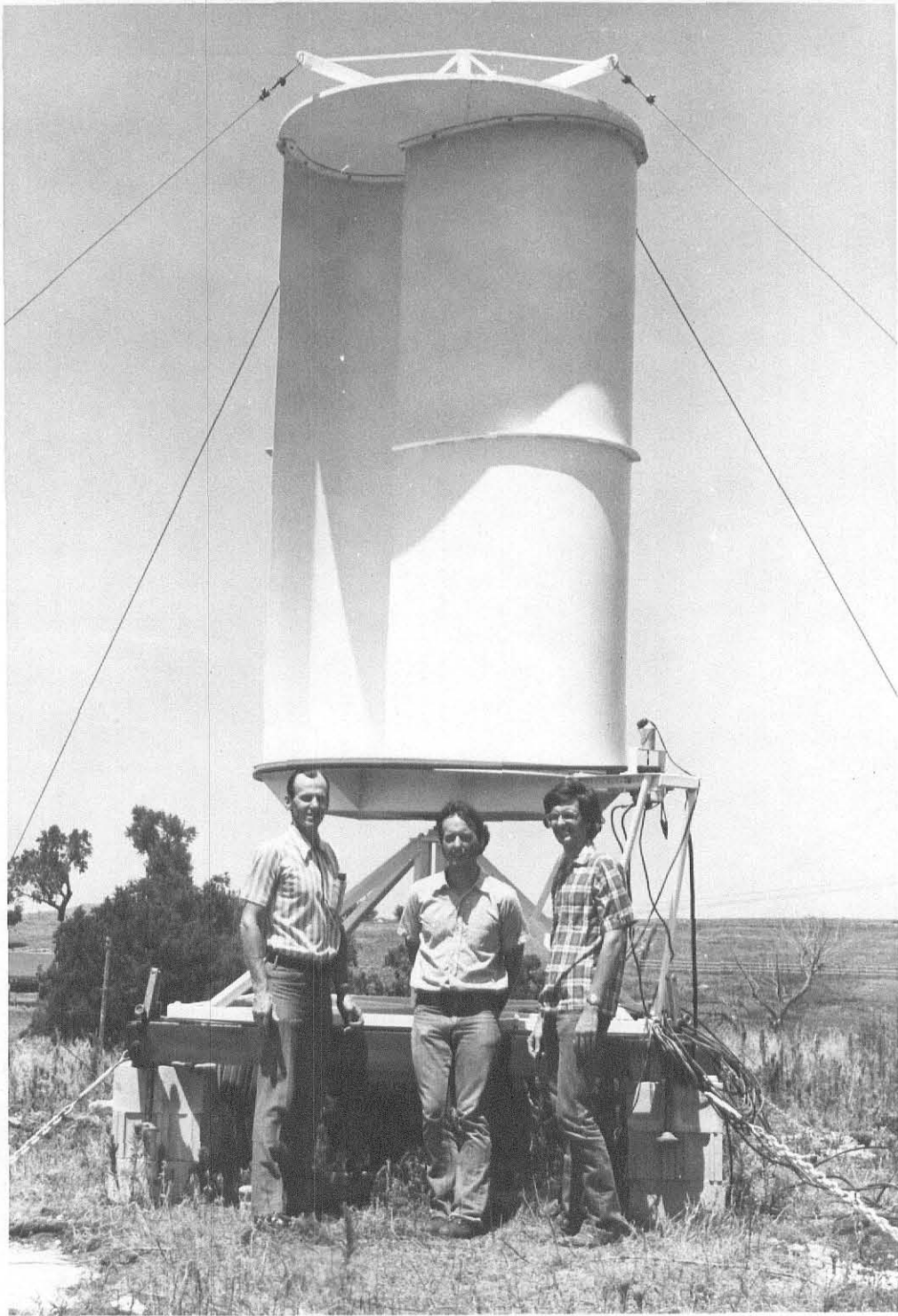


Figure 1: KSU Wind Rotor

alternator shaft was increased to about one hundred eighty degrees by use of idler pulleys, slippage of the belt occurred during some test runs. A flat belt was used for all except the last test when a V-belt was used.

C. ALTERNATOR

A GM automobile alternator, rated at approximately one KW, was used as a load during the experimental testing of the wind rotor. This type of alternator has six diodes as rectifiers instead of a commutator and brush assembly. The field winding of the alternator was supplied with a constant field current during all tests. The electrical output of the alternator was connected to an adjustable load resistance.

CHAPTER III

EXPERIMENTAL TESTING

In July 1975 the KSU Savonius wind-electric power generating system was tested on the KSU campus at a site approximately one mile north of Seaton Hall, the KSU engineering building. The site used was on the top of a hill with excellent access to the prevailing winds. Figure 2, a block diagram of the instrumentation used, shows that the variables measured during the test were wind speed, wind rotor RPM, alternator RPM, and load voltage and current. Because the measured variables were non-steady state in nature, all were recorded on a strip chart except wind rotor RPM. In addition, sampled values of wind speed, rotor RPM, alternator RPM, and load voltage and current were punched on a paper tape every two seconds.

A. DETAILS OF TEST SET-UP

A revolving cup electric anemometer was used to measure wind speed. The electrical output signal from the anemometer was connected to one channel of a four channel strip chart recorder, thus giving a continuous record of wind speed as a function of time. Also, the output signal was sampled every two seconds and the values punched on a paper tape.

To measure wind rotor RPM, a disc having forty two slots was mounted on the wind rotor shaft. A photocell and a light source were located on opposite sides of the slotted disc, so that the interrupted light produced, by means of a photocell, electrical impulses which were applied to a frequency-meter which generated a square wave from the pulse voltage and

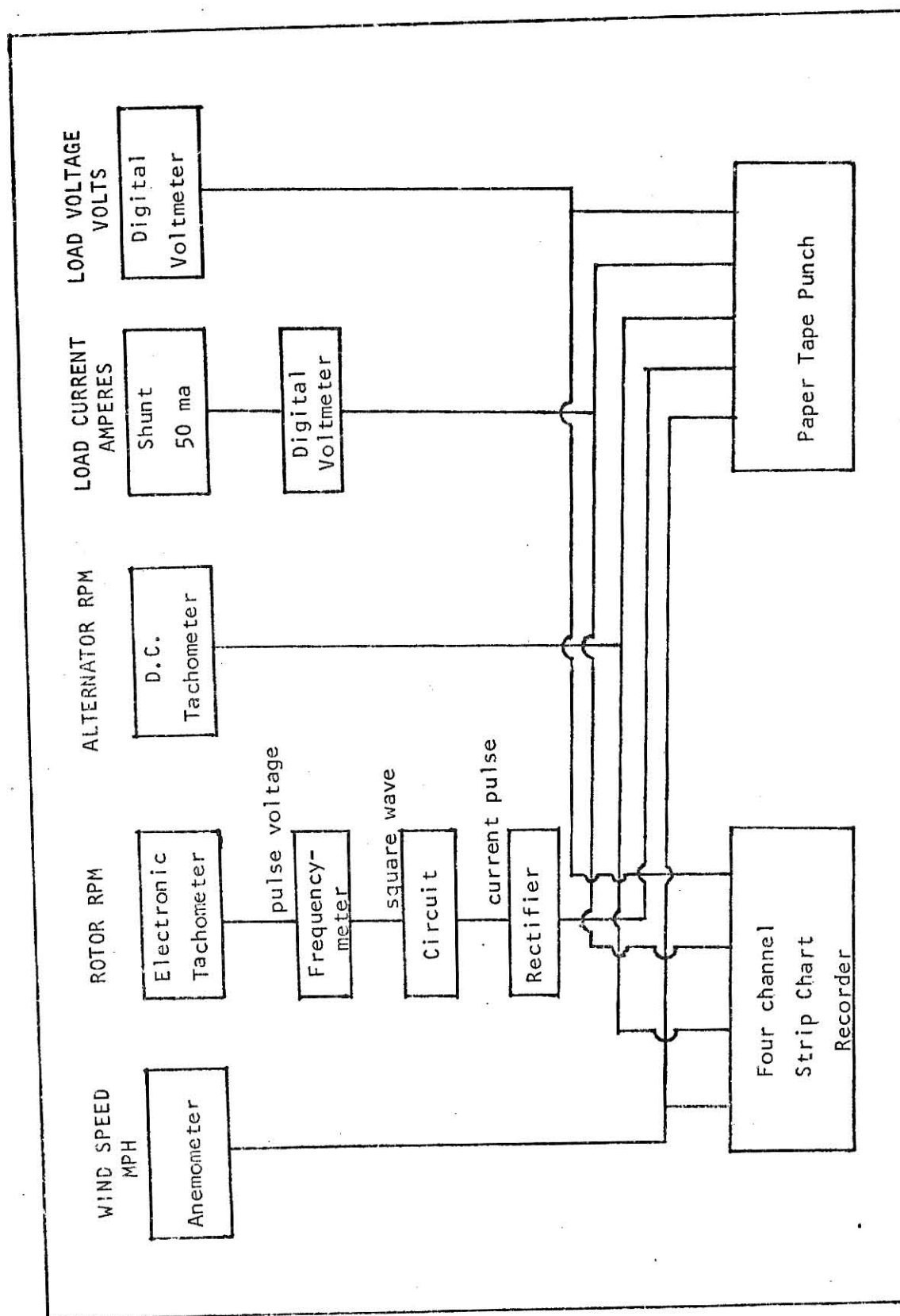


Figure 2. BLOCK DIAGRAM OF INSTRUMENTATION FOR MEASUREMENT OF WIND SPEED, ROTOR RPM, ALTERNATOR RPM AND LOAD CURRENT AND VOLTAGE.

applied it to a discriminating circuit. A fixed current pulse at each half cycle was produced. These pulses were rectified and sampled every two seconds and the values punched on a paper tape. Thus the values are proportional to the number of pulses per second or frequency.

A d.c. tachometer, coupled directly to the alternator shaft, was used to measure alternator RPM. Its output voltage, directly proportional to alternator RPM, was connected to one channel of the strip chart recorder. The output voltage was also sampled every two seconds and values punched on the paper tape.

The voltage drop across a fifty milliohms shunt inserted in the lead wire, which connected the positive terminal of the alternator to the load terminal, was measured. And this measured voltage was used to calculate the load current by applying Ohm's law. The load voltage was monitored using a digital voltmeter. The approach to digital voltage measurement was by employing voltage-to-frequency conversion method. In this method the input voltage determines the rate or frequency at which a series of pulses is generated. This pulse train is gated to a counter for a prescribed, fixed time interval, and the number of pulses counted during this time is a measure of the unknown voltage. Values of load voltage and current were punched every two seconds on the paper tape and strip chart recordings were also obtained.

B. TESTING PROCEDURE USED

The alternator was loaded by a known setting of resistance and data was collected for ten minutes. Then a different setting of load resistance was used and another test run made. Data were obtained for eight different load resistances. This procedure was repeated each day for approximately

two weeks. A total of thirty-three ten minutes test runs were made during this time interval. Values of wind speed, rotor RPM, alternator RPM, and load current and voltage at the terminals of the load were recorded on a separate paper tape for each test run. Strip chart recordings for each test run were also obtained. In addition, the load resistance, in ohms was calculated during each test run.

CHAPTER IV

REDUCTION AND ANALYSIS OF DATA

From the strip chart recordings, time intervals of approximately constant alternator RPM and hence approximately constant wind rotor RPM were identified. The punched paper tape data, i.e. values of wind speed, rotor RPM, alternator RPM, and load voltage and current, taken every two seconds, were then used to calculate the average mechanical power developed by the wind rotor for that "steady state" interval. A total of ninety-one "steady state" intervals were identified ranging in length from ten to seventy seconds. The load current and voltage were the measured variables for calculating the output of the alternator in watts. To calculate the mechanical power required to drive the alternator rotor shaft, the electrical losses in alternator, and mechanical friction and windage losses were added to the electrical power output of the alternator.

The electrical power loss in the alternator as a function of alternator rotor RPM and load current; and mechanical friction and windage loss as a function of alternator rotor RPM were previously determined by Kimball and Jeter(4). Using experimental data and curve fitting techniques, they obtained the following equations to describe these losses:

$$P_{\text{elect}} = a (I_L)^b \quad 4-1$$

where

$$a = 0.7686 - 0.4871 \times 10^{-3} N_a + 0.4172 \times 10^{-7} N_a^2 \\ + 0.1398 \times 10^{-10} N_a^3$$

$$b = 1.751 - 0.5646 \times 10^{-4} N_a + 0.2527 \times 10^{-6} N_a^2 \\ - 0.4241 \times 10^{-10} N_a^3$$

N_a = alternator rotor speed, RPM

And,

$$P_{fw} = -2.88 + 0.807 \times 10^{-2} N_a + 0.2026 \times 10^{-4} N_a^2 \\ + 0.2629 \times 10^{-9} N_a^3 \quad 4-2$$

The useful power output of the alternator is the product of the load current and voltage.

$$P_{out} = V_L I_L \quad 4-3$$

The mechanical power developed by the wind rotor, assuming one hundred percent belt drive efficiency and neglecting bearing friction, is given by equation 4-4.

$$P_{mech} = P_{out} + P_{fw} + P_{elect} \quad 4-4$$

The tip speed ratio is defined as the tip velocity of the wind rotor in MPH divided by the wind speed in MPH, or

$$TSR = \frac{U}{V_w} \quad 4-5$$

Where,

$$U = 0.20527 N_r \\ N_r = \text{wind rotor speed, RPM} = \frac{N_a}{16}$$

The coefficient of power is defined as the ratio of the mechanical power developed by the wind rotor to the theoretical power that can be developed from the wind, or

$$C_p = \frac{P_{\text{mech}}}{P_{\text{wind}}} \quad 4-6$$

Where,

$$P_{\text{wind}} = 0.005AV_w^3 \quad (\text{for air at } 70^\circ \text{ F and } 14.7 \text{ psia})$$

The average value of C_p for each of the ninety one "steady state" intervals mentioned earlier in this chapter was calculated on a NOVA minicomputer using equations 4-1 through 4-6. Figure 3 is a sample of the calculated results for a typical "steady state" interval.

The results were arranged into one MPH "bins" based on average wind speed. For example, all results for average wind speeds greater than ten but less than eleven MPH were grouped in one "bin"; all results for average wind speeds greater than eleven MPH but less than twelve MPH into another "bin", etc. This resulted in an adequate number of data points in the wind speed range ten to sixteen MPH that graphs of coefficient of power versus tip speed ratio could reasonably be drawn for each "bin" of data. There were only a few data points in the wind speed range sixteen to twenty MPH, therefore it was more difficult to graph these.

The data points from the "bin" for wind speeds greater than fourteen MPH but less than fifteen MPH are plotted in Figure 4 with a "best fit" smooth curve drawn in for each wind speed interval for the range of primary interest, i.e. where the coefficient of power is maximum. Similarly, smooth curves were also drawn for the data for the other nine wind speed intervals from eleven to twenty MPH.

Figure 5 shows all ten curves for the ten to twenty MPH wind speed range. From figure 5 it appears that the maximum coefficient of power for the KSU S-rotor is about thirty one percent at a wind speed of approximately 16.5 MPH and a tip speed ratio of one. Furthermore, the maximum coefficient

**THIS BOOK
CONTAINS
NUMEROUS PAGES
WITH THE ORIGINAL
PRINTING BEING
SKEWED
DIFFERENTLY FROM
THE TOP OF THE
PAGE TO THE
BOTTOM.**

**THIS IS AS RECEIVED
FROM THE
CUSTOMER.**

START 197 END 206

START PAPER TAPE. . .

WIND SPEED	VOLTAGE	CURRENT	GEN. RPM	ROTOR RPM
13.556	14.872	15.073	1680.82	102.852
14.037	14.872	15.073	1680.82	102.352
15.961	14.872	15.796	1680.82	102.352
16.442	14.372	15.796	1680.82	102.352
16.442	14.872	15.073	1680.82	99.995
15.961	14.372	15.796	1627.86	99.995
15.961	14.872	14.36	1680.82	102.852
17.404	14.372	15.796	1680.82	102.352
17.404	14.872	16.514	1680.82	99.995
15.961	14.872	15.796	1680.82	102.352

RMC WIND SPEED 15.999 MEAN 15.913 STD DEV 1.251

P MECH	MEAN 350.85	STD DEV. 13.2
P WIND	MEAN 1198.74	STD DEV. 264.63

COEF. OF MERIT .293
TIP SPEED RTO 1.309

FIGURE 3 CALCULATED RESULTS FOR A TYPICAL "STEADY STATE"
INTERVAL

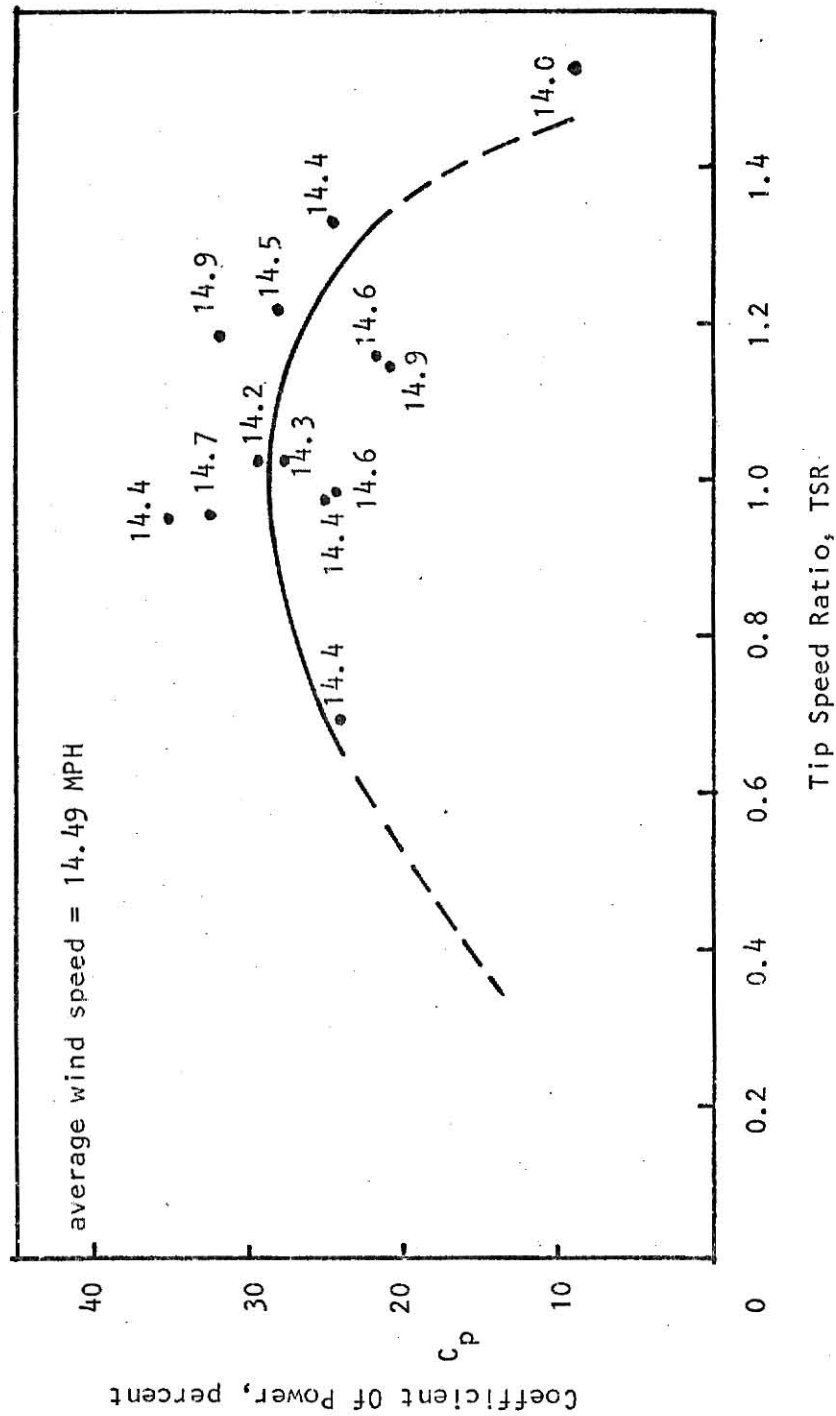


FIGURE 4. GRAPH OF DATA POINTS FROM THE "BIN" FOR WIND SPEEDS $14 < V_w < 15$

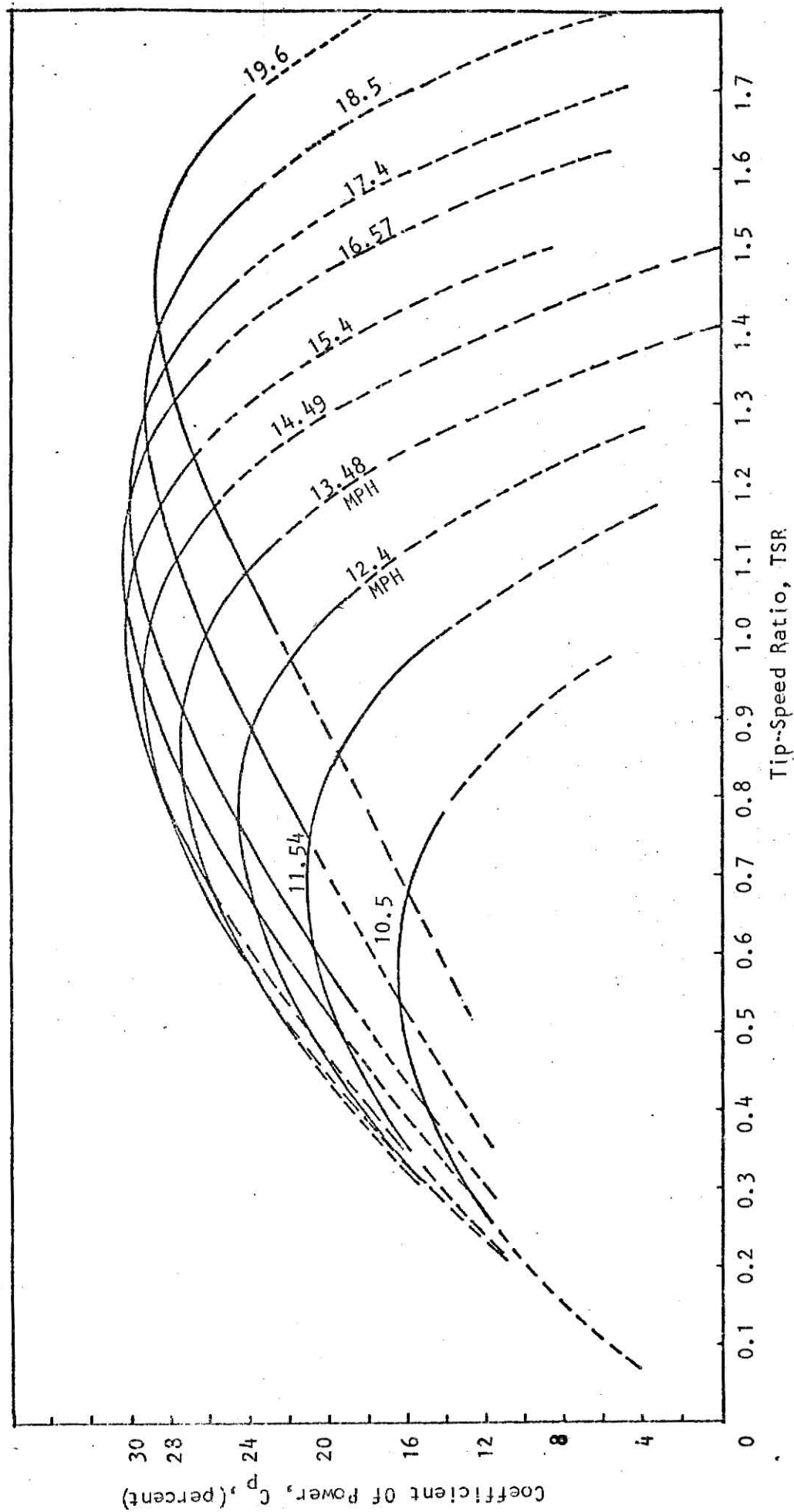


FIGURE 5. COEFFICIENT OF POWER versus TIP SPEED RATIO FOR DIFFERENT WIND SPEEDS

of power for wind speeds greater than 16.5 MPH occurs at increasing values of tip speed ratio and decreases gradually from the maximum of thirty one percent.

It should be remembered, when examining figure 5, that the effects of belt slippage and bearing friction have been neglected, therefore, the power actually developed by the wind rotor is somewhat greater than accounted for by figure 5. The KSU Savonius wind rotor shows good performance for wind speeds greater than 13.5 MPH if operated at the proper tip speed ratios. The coefficient of power can be assumed approximately thirty percent for wind speeds from fourteen to eighteen MPH and tip speed ratios from 0.9 to 1.35.

CHAPTER V

MATHEMATICAL MODELLING

A wind rotor-alternator electric power generating system can be simulated by mathematical models which describe the static and dynamic performance characteristics. First the modelling of static characteristics will be considered, then the modelling of dynamic characteristics.

A. STATIC CHARACTERISTICS

For the coefficient of power versus tip speed ratio characteristic it was desired to establish a mathematical formula defining the coefficient of power as a function of tip speed ratio and wind speed. The curves of C_p versus TSR shown in figure 5 of chapter IV were used as the source of data points for the AARDVARK and STEPDEL computer programs available at the KSU statistical laboratory.

The KSU version of AARDVARK runs under two basic modes of analysis; analysis of variance of balanced data, including covariance analysis of balanced data, and regression analysis. The STEPDEL program performs usual simple and multiple regression analysis and, as an option, provides for building the "best" regression model by successively dropping variables from the regression model that do not contribute sufficient information to the dependent variable. The full model, including all specified independent variables, is fitted and the least significant variables are dropped until all remaining variables are significant at the level specified by the user of the program.

The C_p versus TSR curves represent a non-linear surface. The surface

is non-linear along both horizontal directions (tip speed ratio and wind speed). Therefore, a nonlinear mathematical model containing tip speed ratio and wind speed as independent variables is first assumed. This model then relates the dependent variable, coefficient of power, with tip speed ratio and wind speed. The assumed mathematical model and data points obtained from the curves of C_p versus TSR were supplied to the AARDVARK and STEPDEL computer programs. The maximum and minimum number of independent variables (tip speed ratio, wind speed and variables obtained by transformation) are specified. The AARDVARK computer program results include the correlation matrix, coefficient for the model, values of R-squared, multiple correlation coefficient (r), F-value, and standard error for each of the independent variables between and including the specified maximum and minimum numbers of independent variables.

The mathematical model obtained for the static performance characteristic of the KSU wind rotor is given by equation 5-1.

$$C_p = A + b_2X_2 + b_3X_3 + b_4X_4 + b_5X_5 + b_6X_6 + b_7X_7 + b_8X_8 + b_9X_9 \quad 5-1$$

where,

$$A = -0.0882718$$

$$b_2 = 3.6194063$$

$$b_3 = 0.003341$$

$$b_4 = -20.24582$$

$$b_5 = -3.8756323$$

$$b_6 = 0.0079651$$

$$b_7 = -1.4449625$$

$$b_8 = -0.11441177$$

$$b_9 = 64.5027$$

$$X_2 = \text{TSR} \quad (0 < \text{TSR} < 2.0)$$

$$X_3 = V_w \quad (10.5 < V_w < 19.6)$$

$$X_4 = \frac{X_2}{X_3}$$

$$X_5 = X_4 X_2$$

$$X_6 = X_2^4 X_3$$

$$X_7 = \frac{X_6 X_2}{X_3^2}$$

$$X_8 = X_2 X_3$$

$$X_9 = \frac{1}{X_3^3}$$

The value of R-squared, $r(R)$, standard error and F-value for equation 5-1 are as follows:

$$\text{R-squared} = 0.9743 \quad (\text{dimensionless})$$

$$r = 0.9871 \quad (\text{dimensionless})$$

$$\text{standard error} = 0.01506 \quad (\text{dimensionless})$$

$$\text{F-value} = 1474.116 \quad (\text{dimensionless})$$

Although R-squared is stated as a percentage, the ratio of the sum of the squares due to regression and the total sum of squares describes a measure to observe the suitability of the model. This value ranges from zero to one. The larger it is, the better the fitted equation models the data. The correlation coefficient, r , is a measure of mutual relationship between variables. In this modelling, however, it was treated as the measure of the degree of closeness of the relationship between independent variables. The value of ' r ' ranges from minus one to plus one. In practical application unity ($r = 1$) is seldom reached but 0.9 and above is not

uncommon.

F, the variance ratio, is in fact the ratio of the two mean squares calculated from deviations from regression and due to regression. This particular value is checked using a table first tabulated by Fisher(11) in 1920. These tables are tabulated at one, five and ten percent level of significance. Tests of significance have the property that if the null hypothesis is true the probability of obtaining a significant result has a known value which is one, five or ten percent. In the present analysis the F-value is far greater than 1.94 (the table value for five percent level of F-distribution). Similarly, even at a level of one percent the F-value is far greater than the table value of 2.51. Thus the F-value is significant at both levels.

It should be emphasized, however, that raw data values were not used; the source of data was the curves in Figure 5.

The torque developed by the wind rotor can be obtained by rearranging equation 4-6 into the following form (equation 5-1 can be used for C_p):

$$T_{dev} = \frac{2.0601 C_p V_w^3}{N_r} \quad 5-2$$

Figure 6 shows the torque characteristics of the wind rotor as a function of rotor RPM for given wind speeds. Equation 5-2 is not valid for zero RPM rotor speed, and wind speeds less than ten MPH and greater than twenty MPH. The values of torque developed at zero rotor speed for a given wind speed (stall torque) were obtained by extrapolating the curves. In the region of primary interest the curves are approximately parallel and equally spaced, and are like those of two phase a.c. servomotor.

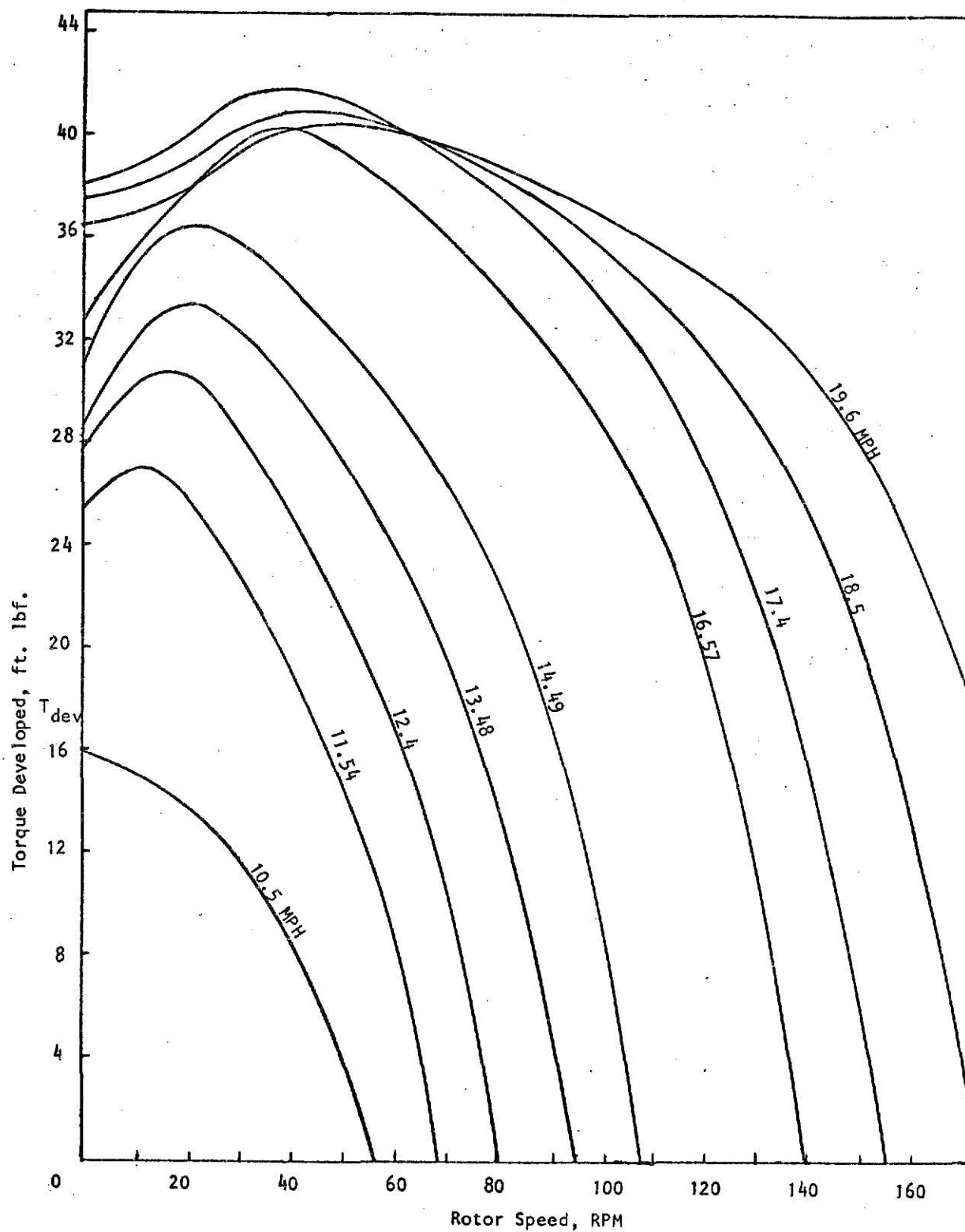


FIGURE 6. WIND ROTOR TORQUE-SPEED CHARACTERISTICS

B. WIND ROTOR-ALTERNATOR SYSTEM DYNAMICS

Figure 7 shows mechanical and electrical schematics of the wind-electric power generating system. For the automotive alternator it was assumed that the field current is constant and that the effect of armature reaction on induced e.m.f. is negligible. The alternator was rated at approximately one KW. For this machine the electrical time constant as obtained from the strip chart recordings for the load current and alternator RPM is approximately 0.1 seconds. Therefore it was assumed that:

$$T_a = \frac{L_a}{R_a + R_L} = 0.1 \text{ seconds} \quad 5-3$$

The inertia of the alternator rotor and the damping in the rotating part of the alternator were both referred to the wind rotor shaft speed. The equivalent inertia and damping of the wind rotor-alternator system's rotating parts are as follows:

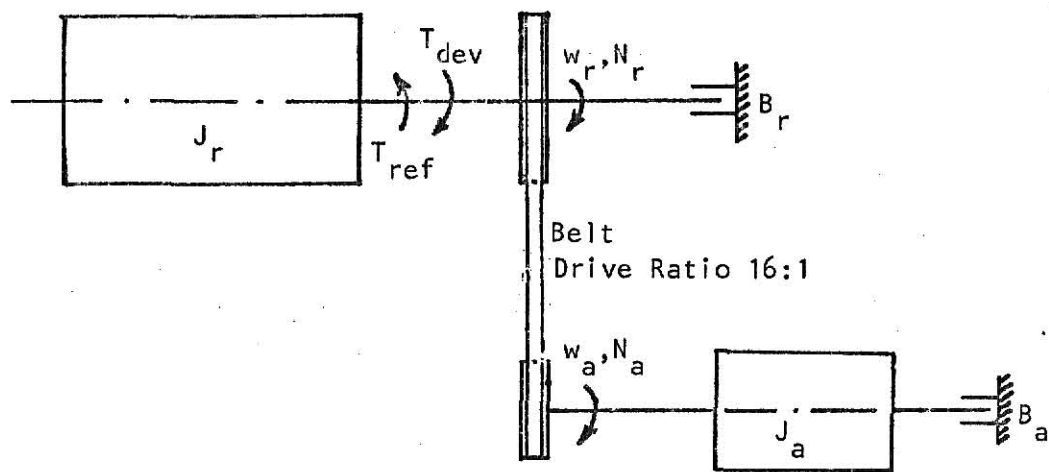
$$J_{eq} = J_r + \left(\frac{D_r}{D_a} \right)^2 J_a \quad 5-4$$

And

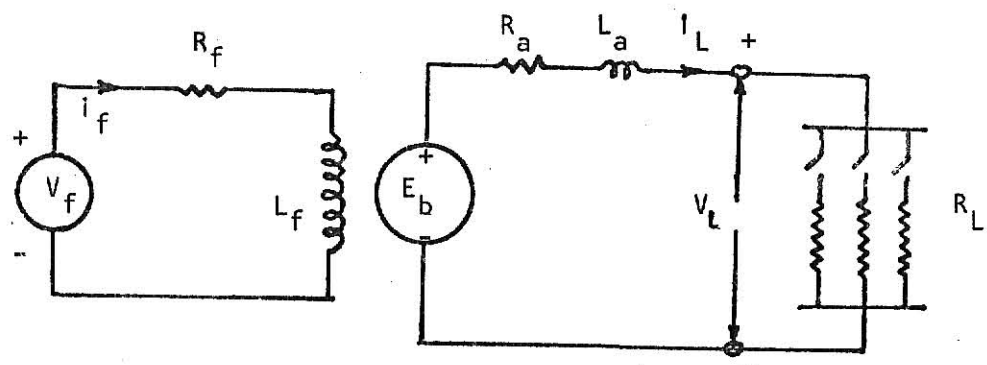
$$B_{eq} = B_r + \left(\frac{D_r}{D_a} \right)^2 B_a \quad 5-5$$

Where,

D_a	= diameter of pulley on rotor shaft,	inches
D_r	= diameter of pulley on alternator shaft,	inches
J_a	= inertia of alternator rotor,	lb. ft. sec ²
J_r	= inertia of wind rotor,	lb. ft. sec ²
B_r	= damping coefficient of wind rotor,	lb. ft. sec
B_a	= damping coefficient of alternator rotor	lb. ft. sec



(a) Mechanical System (rotating mass and friction)



(b) Electrical System (field and armature circuit)

FIGURE 7. SCHEMATIC OF WIND-ELECTRIC POWER GENERATING SYSTEM

Inspection of strip chart recordings shows that a reasonable value for the mechanical time constant is approximately 1.5 seconds. From the rotor's acceleration point of view in the region of primary interest it is reasonable assumption that:

$$T_r = \frac{J_{eq}}{B_{eq}} = 20.0 \text{ seconds} \quad 5-6$$

Equation 5-4 contributes to the kinetic energy storage of rotating mass system and equation 5-5 to the energy dissipation term in D'Alembert's law. It was assumed that the belt slippage was negligible. Applying D'Alembert's principle at a point on the wind rotor shaft near the vanes and assuming that the shaft is perfectly rigid, results in the following equation:

$$J_{eq} \frac{d\omega_r}{dt} + B_{eq} \omega_r + T_{ref} - T_{dev} = 0.0 \quad 5-7$$

The independent variable in the above equation is time, t , and the angular velocity of the rotor, ω_r , is the dependent variable. The coefficients are assumed to be time invariant, and independent of angular velocity, therefore the equation is linear. But torque developed by the wind rotor is dependent on the angular velocity (see equation 5-2) of the wind rotor and thereby introduces nonlinearity in the above equation.

Applying Kirchoff's second law to the armature circuit of the alternator results in the following equation:

$$L_a \frac{di_L}{dt} + R_a i_L + V_L - E_b = 0.0 \quad 5-8$$

The first term in the above equation is the voltage drop due to the inductance of the armature winding, the second term is the voltage drop due to the resistance of the armature winding, the third term is the voltage drop across the load resistance, and the fourth term is the back e.m.f.

voltage. The voltage drop of the leads connecting the alternator to the load resistance was assumed negligible.

The torque reflected to the wind rotor shaft by the alternator is given by the following equation:

$$T_{ref} = \frac{(P_{out} + P_{elect} + P_{fw}) 550}{745.7 W_r} \quad 5-9$$

In the above equation, the power required to overcome the friction, P_{fw} , is included. However, when this equation is substituted in equation 5-7, the second term of equation 5-7 takes care of the friction and windage loss for the alternator rotating parts. The friction loss in the wind rotor is also included in the equivalent damping, B_{eq} .

The automotive type alternator used was calibrated in the EE laboratory by Jeter and Kimball(4) and then they obtained a relationship for the open circuit voltage as a function of alternator rotor RPM. If it is assumed that the induced e.m.f. is equal to the open circuit voltage, V_{oc} , and that the effect of armature reaction on the induced e.m.f. is negligible, then the back e.m.f., E_b , is given by the following equation:

$$E_b = V_{oc} = -0.806 + 0.01322 N_a - 0.6 \times 10^{-7} N_a^2 \quad 5-10$$

The terminal voltage, V_L , is obtained using Ohm's law, or

$$V_L = I_L R_L \quad 5-11$$

This chapter has been concerned with defining the static and dynamic performance characteristics of the wind rotor-alternator system by means of mathematical equations. Now, using these equations, both static and dynamic performance of the system be investigated using a digital computer. This will be done in the chapters which follow.

CHAPTER VI

ANALYSIS OF THE STATIC PERFORMANCE CHARACTERISTICS

The load on the wind rotor plays an important role in its performance. Overloading or underloading causes a decrease in the coefficient of power. The operation of the wind rotor at a constant load is discussed first. For the purpose of discussion it is desirable to draw loci of constant load resistance on the C_p versus TSR characteristic.

A. LOCI OF CONSTANT LOAD ON C_p versus TSR CHARACTERISTIC

In order to calculate values of load resistance (in ohms) on the alternator a computer program in FORTRAN IV programming language was written. In this program a reasonable value of alternator armature resistance was assumed first. Using this value of resistance the value of load resistance can be calculated by using equations 4-1, 4-2, 4-3, 4-4, 4-5, 4-6, 5-1, 5-8 (for steady state), 5-10, and 5-11. Equation 5-11 gives the value of load resistance. Equation 5-8, for steady state conditions, was solved to obtain load voltage, V_L . Using this value of load voltage and equation 4-3 the load current, I_L , was calculated. Then the electrical loss in the armature circuit calculated by using equation 4-1 is compared with loss calculated from $I_L^2 R_a$ formula. The value of armature resistance was so selected that the difference obtained was minimum. This procedure of calculating load resistance was quite accurate, except for neglecting temperature effect on the armature circuit resistance, R_a . The computer program is given in Appendix I.

The values of load resistance, which were calculated by the procedure described in the previous paragraph were used to draw loci of constant load resistance on the coefficient of power versus tip speed ratio characteristic curves. A few loci of constant load are shown superimposed on the C_p versus TSR curves in Figure 8. If the value of load resistance connected to the output terminals of the alternator is assumed to remain unchanged then the system will adjust itself from an initial steady state condition to a new steady state condition. In addition, the electric power will be generated over a wide range of frequencies as there may be a wide range of rotor RPM depending on initial load and final wind speed. At this point three different cases of possible wind rotor-alternator system operation can be studied. These three cases are as follows:

Case I: Operation at constant load

Case II: Operation at maximum coefficient of power

Case III: Operation at constant speed

B. CASE I: OPERATION AT CONSTANT LOAD

The main aim was to select values of load resistance, for different wind speeds such that the coefficient of power would always be within some tolerable limit of its maximum at different wind speeds. Here a tolerance of two percent was selected, i.e., the coefficient of power will remain within two percent of its maximum possible value for a given wind speed. For each wind speed Table I gives the maximum C_p and the two extreme values of tip speed ratio and load resistance for two percent deviation from the maximum coefficient of power. Table I gives the values of tip speed ratio and load resistance at maximum C_p . From Table I it appeared that if a

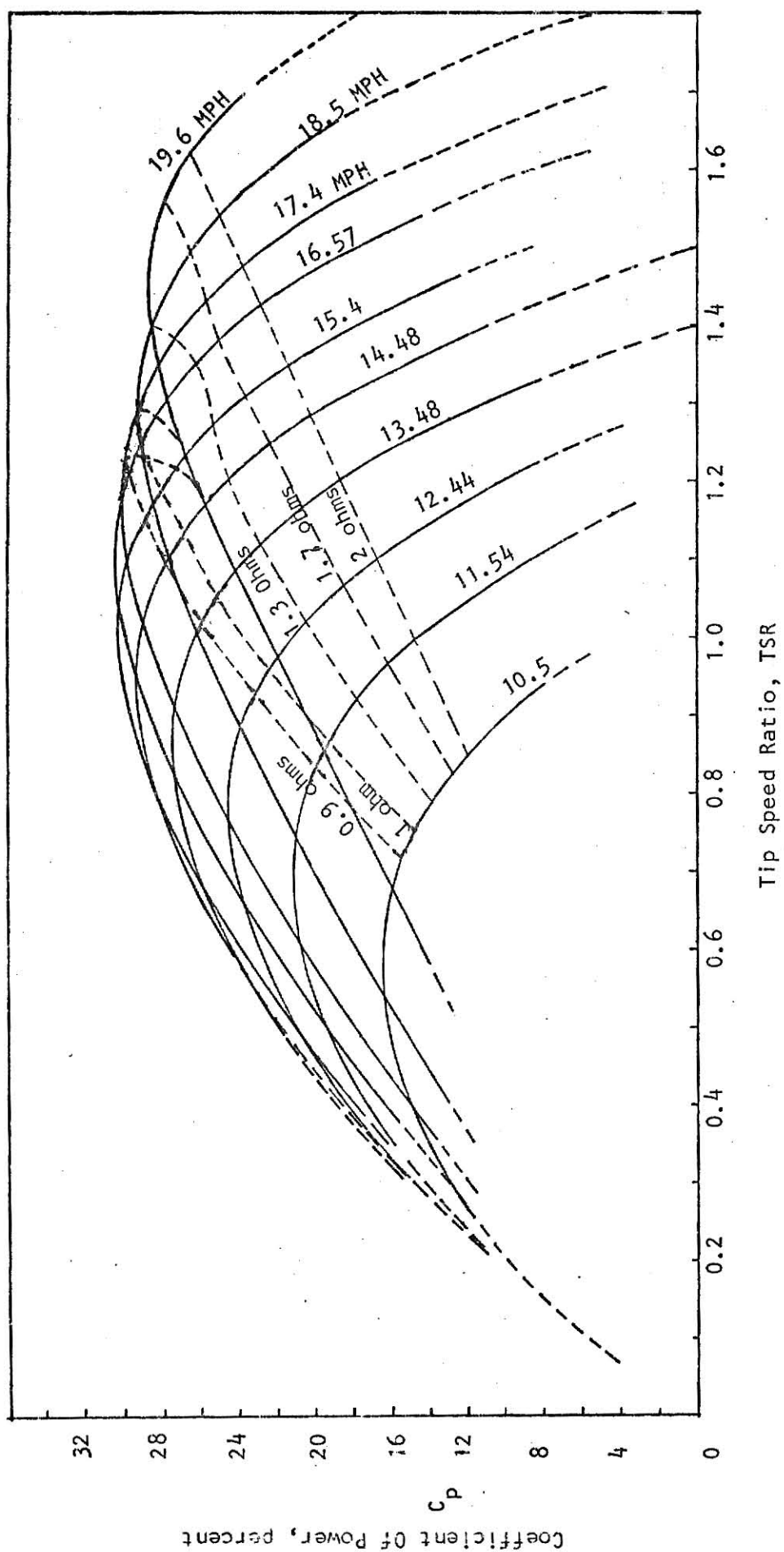


FIGURE 8. LOCI OF CONSTANT LOAD RESISTANCE ON C_p versus TSR CHARACTERISTIC

V_w (MPH)	C_{p-max} (%)	TSR @ C_{p-max}	R_L @ C_{p-max} (ohms)	TSR RANGE FOR $C_{p-max} -2\%$	R_L RANGE FOR $C_{p-max} -2\%$ (ohms)
10.51	16.44	0.65	0.43	0.5-0.75	0.22-1.03
11.54	21.10	0.75	0.48	0.6-0.85	0.27-0.92
12.44	24.51	0.85	0.52	0.7-0.95	0.34-0.95
13.48	27.48	0.90	0.57	0.75-1.05	0.33-0.99
14.49	29.36	1.00	0.65	0.85-1.10	0.40-1.00
15.41	30.24	1.05	0.67	0.90-1.20	0.43-1.07
16.57	30.41	1.15	0.80	1.00-1.30	0.54-1.22
17.40	30.0	1.25	0.97	1.10-1.35	0.68-1.26
18.50	29.2	1.35	1.16	1.20-1.45	0.86-1.47
19.60	28.7	1.45	1.49	1.30-1.65	1.07-2.14

TABLE I

LOAD RESISTANCE FOR MAXIMUM COEFFICIENT OF POWER
OPERATION

value of load resistance between 0.9 ohms and one ohm is selected then the deviation in the C_p from its maximum value (at a given wind speed) will be within two percent for each wind speed in the ten to eighteen MPH range.

C. CASE II: OPERATION AT MAXIMUM COEFFICIENT OF POWER

To always obtain maximum coefficient of power, regardless of wind speed, it would be necessary to automatically adjust the value of load resistance as the wind speed varies. The values of load resistance have already been given in Table I. Figure 9 shows that the relationship between load resistance and wind speed, for maximum coefficient of power operation, is slightly parabolic.

A combination schematic and block diagram for a feedback control system to regulate the load for maximum C_p operation is shown in Figure 10. In this feedback scheme the value of load resistance is compared with the desired value of load resistance (set point) which is a function of wind speed. The error signal, whenever present, would be the input to a servo type actuator which would either increase or decrease the load resistance. Such an actuator can be modeled as a second order system.

D. CASE III: OPERATION AT A CONSTANT SPEED

By controlling the wind-electric system to operate at a constant speed, the frequency of the a.c. voltage could be kept constant and it could be connected to a utility power grid. However, voltage fluctuations would be present, an undesirable feature for a utility power grid, thereby creating a necessity for voltage stabilizers. To maintain constant speed operation over a given range of wind speeds, it would be necessary to regulate the load.

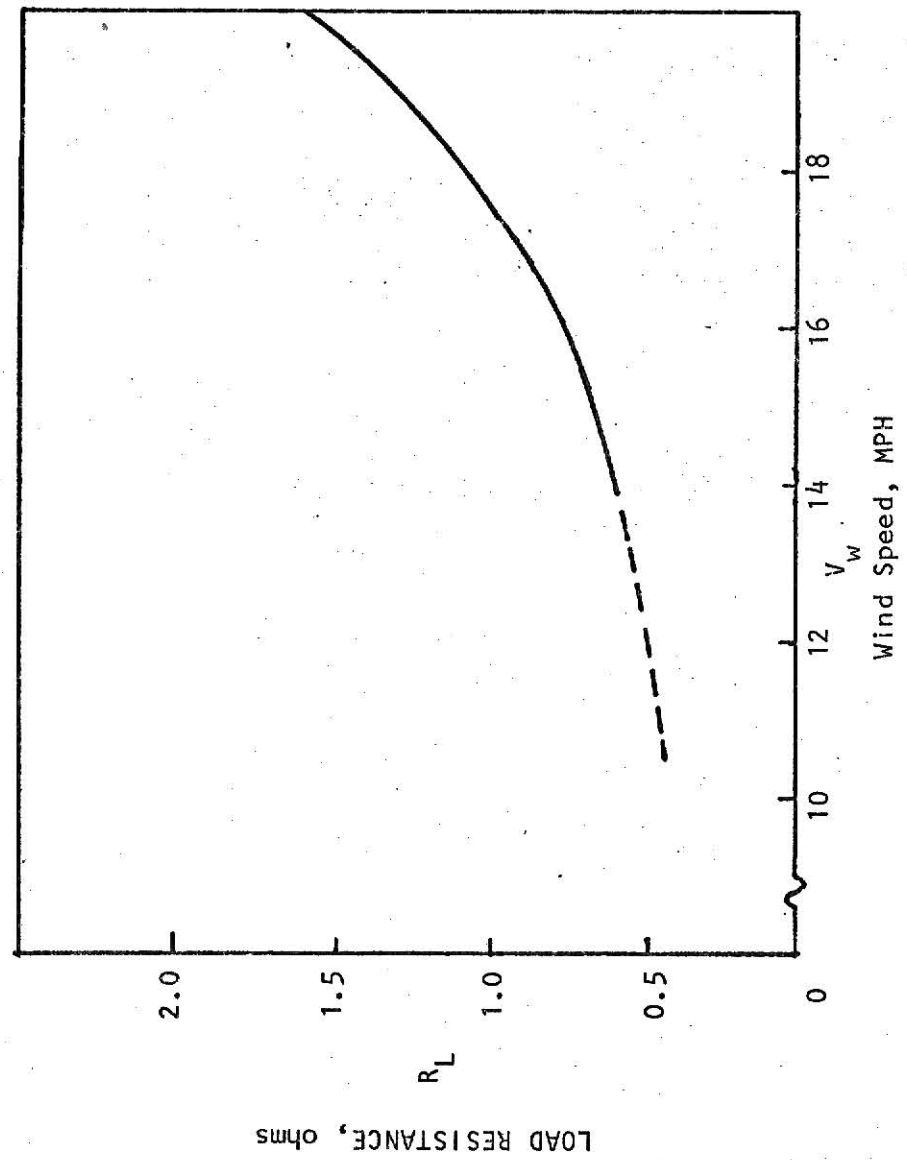


FIGURE 9. LOAD RESISTANCE VERSUS WIND SPEED FOR MAXIMUM C_p OPERATION

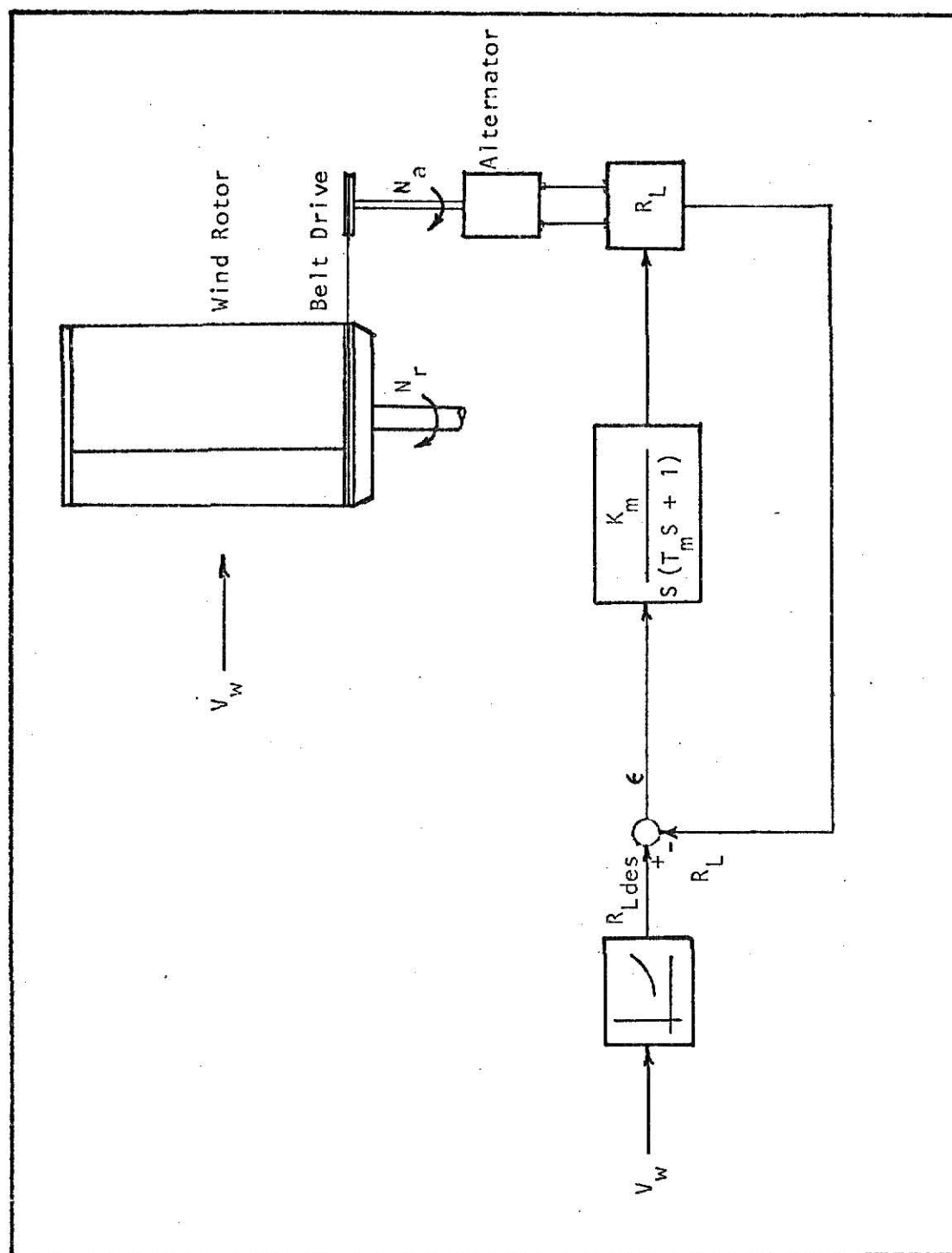


FIGURE 10. REGULATION OF LOAD FOR MAXIMUM COEFFICIENT OF

POWER EXTRACTION

Figure 11 shows loci of constant load resistance superimposed on the torque-rotor RPM characteristics (previously given in Figure 6). Table II gives values of load resistance and coefficients of power if constant speed operation (say $N_r = 60$ RPM) were to be realized, regardless of wind speed. The maximum coefficient of power for the various wind speeds is also included in Table II for comparison purpose. Figure 12 is a graph of desired load resistance as a function of wind speed for constant speed operation. A combination block and schematic diagram representation for a feedback control system to realize constant speed operation is shown in Figure 13. A rotor speed of sixty RPM would be suitable in an area where the average wind speed varies between 11.5 to 19.0 MPH. It should be noted that the maximum reduction in the coefficient of power, for constant speed as opposed to maximum C_p operation, would be approximately eight percent at a wind speed of 17.4 MPH.

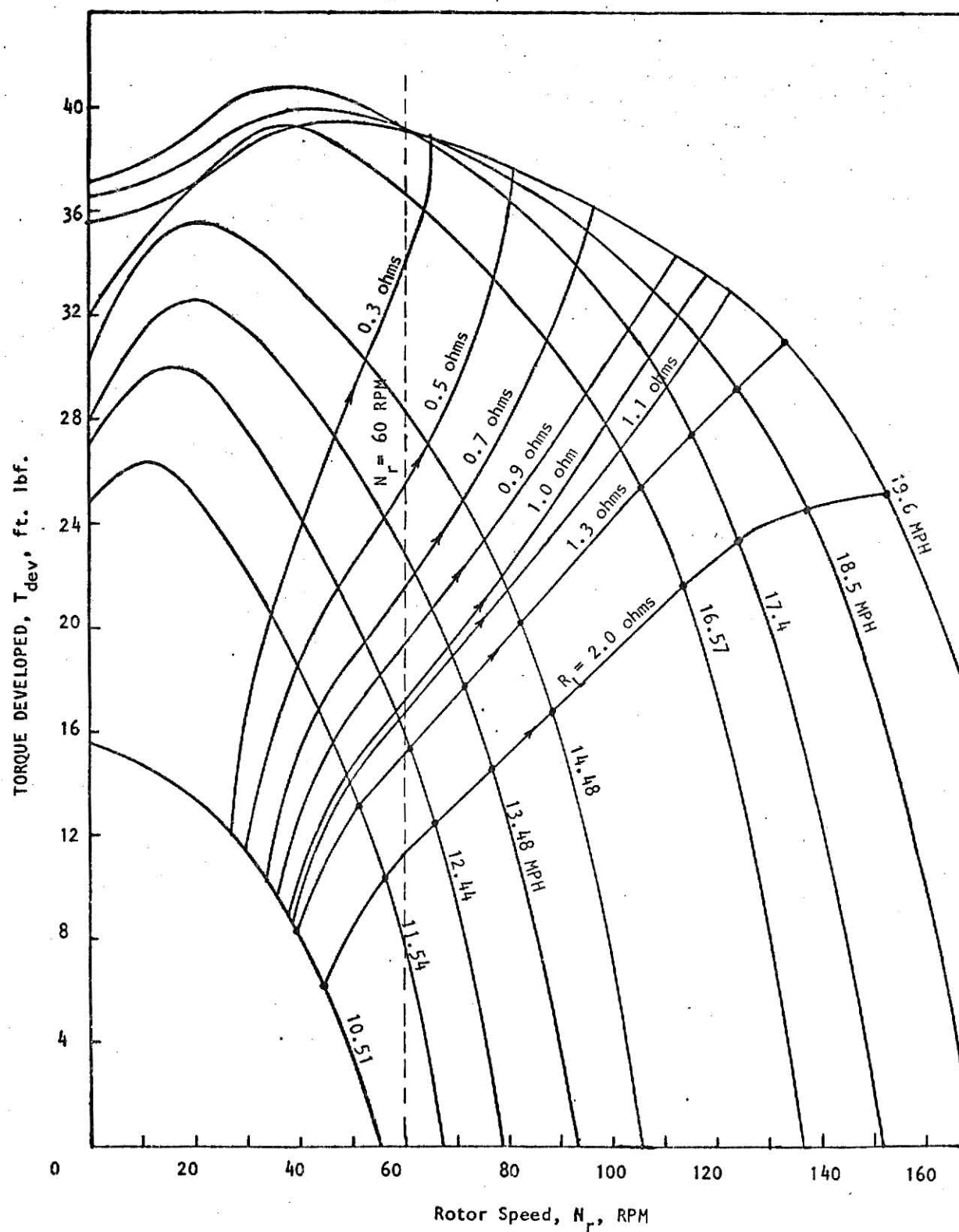


FIGURE 11. TORQUE-SPEED CURVES WITH LOCI OF CONSTANT LOAD RESISTANCE

WIND SPEED (MPH)	LOAD RESISTANCE $N_r = 60$ RPM (ohms)	C_p FOR $N_r = 60$ RPM (%)	C_{p-max} FOR GIVEN WIND SPEED (%)
11.54	3.000	14.0	21.1
12.44	1.170	22.7	24.5
13.48	0.573	27.5	27.5
14.49	0.403	28.4	29.4
15.41	0.311	27.3	30.0
16.57	0.256	25.0	31.0
17.40	0.225	22.0	30.0

TABLE II

WIND ROTOR PERFORMANCE AT A CONSTANT ROTOR SPEED

($N_r = 60$ RPM)

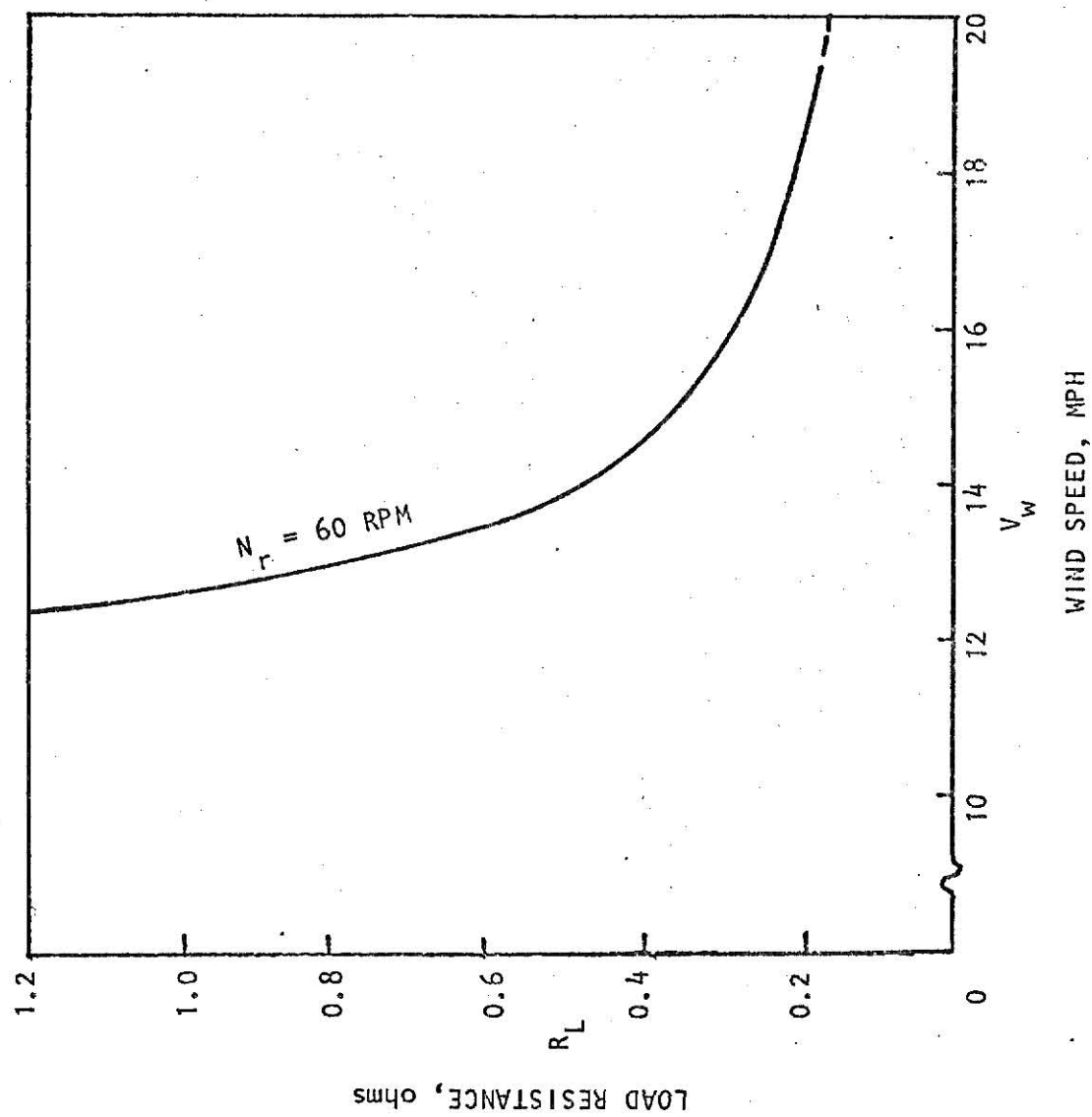


FIGURE 12. LOAD RESISTANCE versus WIND SPEED FOR CONSTANT N_r

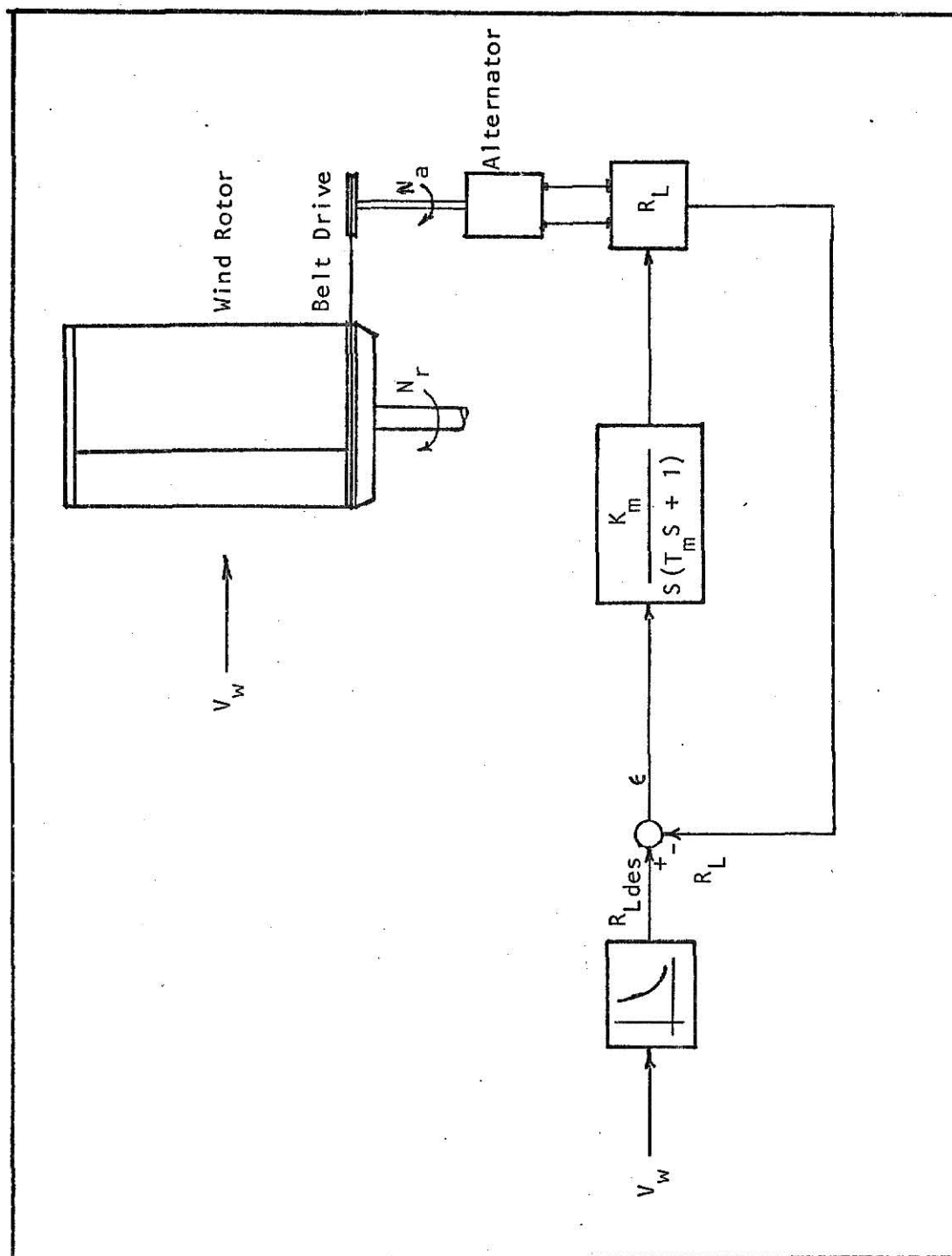


FIGURE 13. REGULATION OF LOAD FOR CONSTANT SPEED OPERATION

$N = \text{CONSTANT}$

CHAPTER VII

TIME-DOMAIN ANALYSIS

The transient response of the wind rotor-alternator system for a step change in wind speed is investigated in this chapter. The response of rotor RPM to a step change in wind speed, for different constant values of load resistance, is studied in order to determine the transient behavior of the rotor at different loads.

A. TRANSIENT RESPONSE

Before the transient response of the wind rotor-alternator system described by differential equations 5-7 and 5-8 could be obtained using a digital computer, it was necessary to rewrite the equations as follows:

Let,

$$\begin{aligned} Y(1) &= \omega_r & \text{and} & & Y(2) &= I_L \\ DY(1) &= \frac{d\omega_r}{dt} & & & DY(2) &= \frac{dI_L}{dt} \end{aligned}$$

Then applying these definitions to equations 5-7 and 5-8 results in the following equations:

$$DY(1) = \frac{(T_{dev} - T_{ref}) - B_{eq} Y(1)}{J_{eq}} \quad 7-1$$

And

$$DY(2) = \frac{E_b - V_L - R_a Y(2)}{L_a} \quad 7-2$$

Also equation 5-9 was rewritten, omitting P_{fw} term since it is already accounted for in equation 7-1, as follows:

$$T_{ref} = \frac{550 (P_{out} + P_{elect})}{745.7 Y(1)} \quad 7-3$$

Next, the initial conditions (for time, $t=0$ sec.) of the system, viz: values of wind rotor RPM, wind speed and load current and voltage had to be specified. Values of all other parameters including load resistance also had to be supplied. Now the transient response of the system to a step change in wind speed could be calculated on a digital computer using the Runge-Kutta-Gill technique. The computer program used is given in Appendix II. This type of problem is a propagation problem with exactly known initial values for a lumped-parameter system.

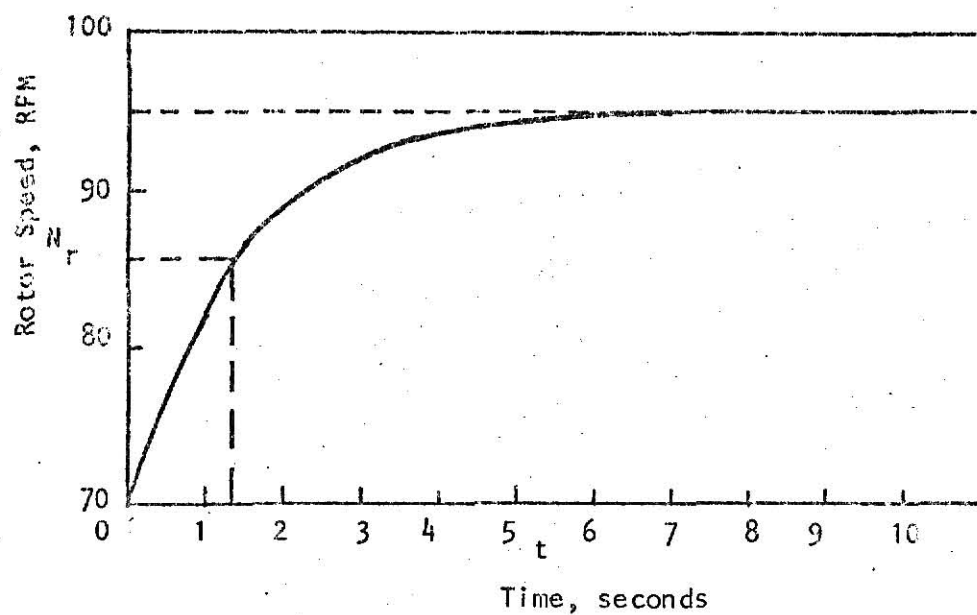
In this study of the transient response the following initial conditions were used.

	$R_L = 0.657$ ohms	$R_L = 1.333$ ohms
Rotor Speed, RPM	70.6	84.725
Wind Speed, MPH	14.488	14.488
Load Current, Amps.	16.152	11.035
Load Voltage, Volts	10.612	14.71

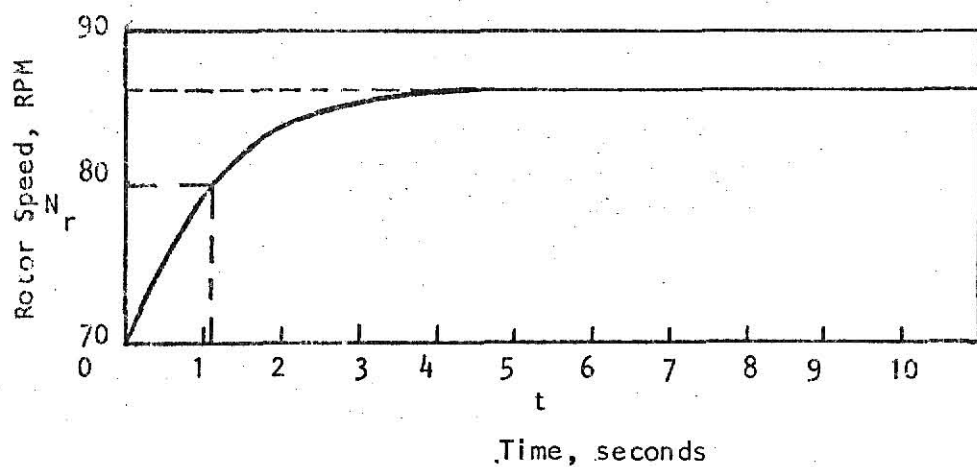
In addition, the following parameter values applicable to the wind rotor-alternator system were used:

$$\begin{aligned} L_a &= 0.022 \text{ henrys} \\ R_a &= 0.22 \text{ ohms} \\ J_{eq} &= 8.2 \text{ lbf.-ft.-sec}^2 \\ B_{eq} &= 0.41 \text{ lbf.-ft.-sec/rad.} \end{aligned}$$

Figure 14 shows the response of wind rotor speed to step changes in wind speed from 14.488 to 16.572 MPH and 14.488 to 18.5 MPH with a 0.675



(a) for step change in wind speed from 14.488 to 18.5 MPH



(b) for step change in wind speed from 14.488 to 16.572 MPH

FIGURE 14. TRANSIENT RESPONSE FOR 0.657 ohms LOAD RESISTANCE

ohms load resistance on the alternator. Figure 15 shows the transient response for the same step changes in wind speed when a load resistance of 1.333 ohms was used. It can be noted that the time to reach 63.2 percent of the total change in the rotor speed when the load resistance was 1.333 ohms is approximately 0.4 seconds greater than when load resistance was 0.657 ohms. Therefore, the effect of increasing load current by decreasing the value of load resistance was to make the response quicker to a step change in wind speed.

B. TRANSFER FUNCTION

With reasonable accuracy, in the range of primary interest, the wind rotor can be modeled as a first order system for changes in rotor speed from some initial rotor RPM. The linearized transfer function, derived in Appendix III, for the wind speed range from eleven to twenty MPH is given by the following equation:

$$\frac{\Delta N_r(S)}{\Delta V_w(S)} = \frac{K_r}{(1.5 S + 1)} + \frac{N_r(0)}{\Delta V_w(S)} \quad 7-4$$

Where,

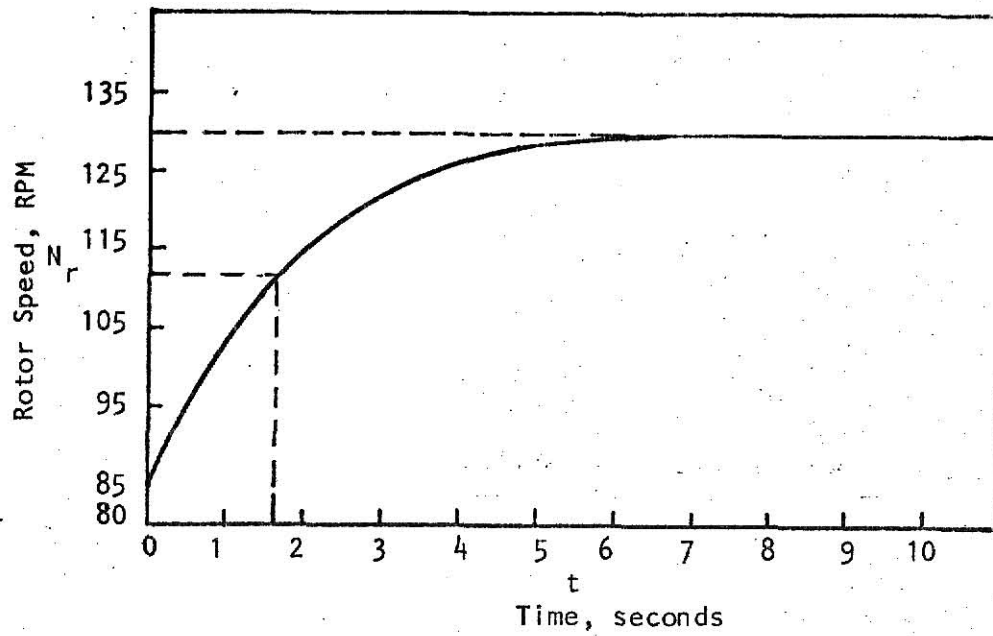
$\Delta N_r(S)$ = Laplace Transform of rotor speed

$N_r(0)$ = Rotor speed at time $t = 0$ second

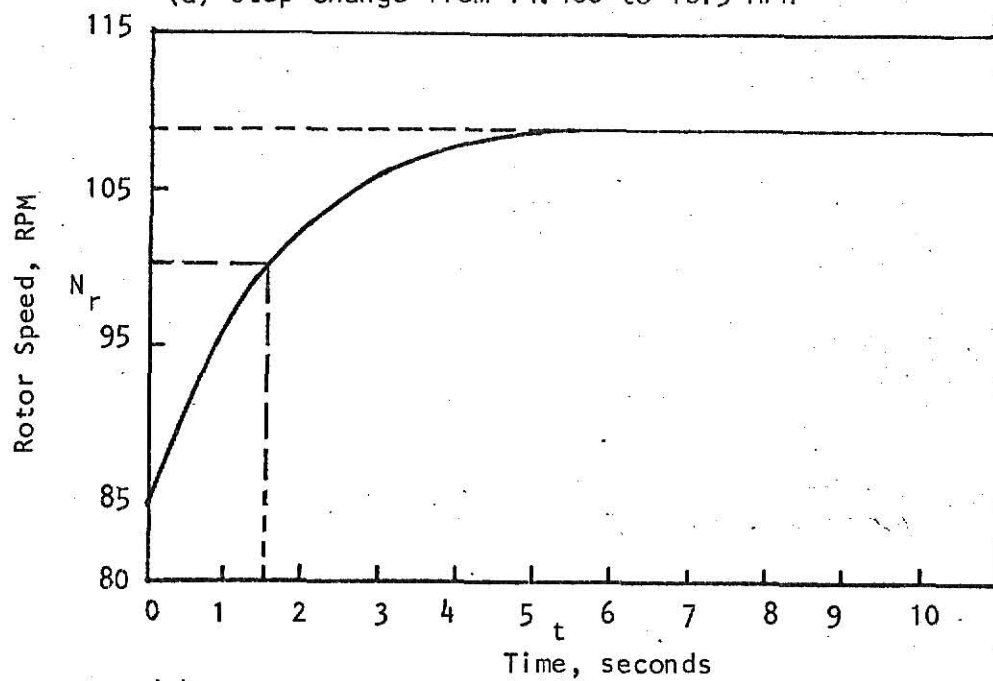
$\Delta V_w(S)$ = Laplace Transform of changes in wind speed

K_r = Wind rotor gain constant

From the transient response curves for step changes in wind speed it can be seen that a time constant of approximately 1.5 seconds is appropriate. This means that wind frequencies higher than $\frac{1}{3\pi}$ Hz will be



(a) step change from 14.488 to 18.5 MPH



(b) step change from 14.488 to 16.572 MPH

FIGURE 15. TRANSIENT RESPONSE FOR 1.333 ohms LOAD RESISTANCE

attenuated, i.e., low frequency components will be reproduced faithfully and high frequency components are both attenuated in amplitude and shifted in phase. In other words, the Savonius wind rotor, although nonlinear, has characteristics of a low pass filter in the range of interest.

The transfer function approximately represents the wind rotor for small step changes of maximum magnitude two MPH. This transfer function is also valid for both positive and negative step changes. The value of rotor gain constant, K_r , can be obtained from Figure 16. Figure 16 represents rotor gain constant as a function of load resistance for five different ranges of wind speed. For step changes from one range to the other one, an average value can be taken for the rotor gain constant. The Savonius rotor has a high inertia compared to its damping and the step response from zero rotor speed is very slow in comparison with that from finite rotor speed in the region of primary interest.

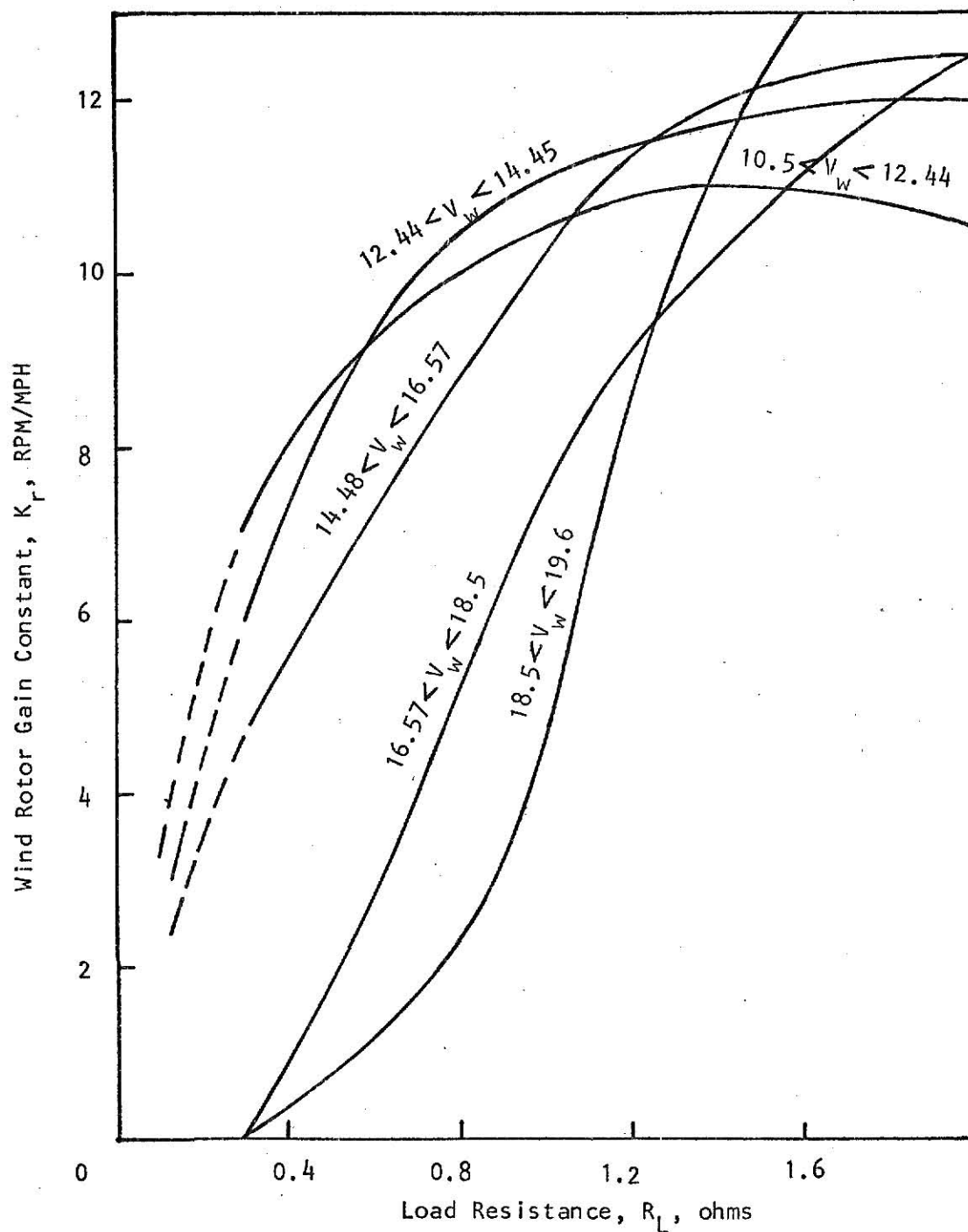


FIGURE 16. WIND ROTOR GAIN CONSTANT versus LOAD RESISTANCE
FOR FIVE WIND SPEED RANGES FROM 10 TO 20 MPH

CHAPTER VIII

CONCLUSIONS AND RECOMMENDATIONS

The static characteristics have been established by using electric generator as a load on the wind rotor. This was a more convenient method for collection of data and it was also useful for studying the behavior of the wind-electric power generating system. The statistical analysis threw light on the accuracy of the static model. Although the effect of armature reaction on induced e.m.f. was neglected and operation of the alternator was assumed to be restricted in the linear range of magnetization curve, the dynamic model is accurate. Thus the simulation of the wind-electric power generating system on a computer yielded accurate response curves, even for step changes as high as four MPH.

For a purely resistive load it is advisable to run the KSU Savonius wind rotor-electric generator system at a load between 0.9 and one ohm. For a constant rotor speed or maximum coefficient of power operation a servo type actuator having property of a low-pass filter can be used. Such an actuator can be a second order system having closed-loop dynamics similar to the dynamics of the wind rotor.

The approximate value of wind rotor inertia is 171 ft.lbf.sec^2 . The slope of rotor torque-speed characteristics in the linear region gave the damping coefficient of the wind rotor as 4.77 ft.lbf.sec . The viscous friction of the wind rotor and the load was approximately 0.04 ft.lbf.sec . Thus the wind rotor time constant approximately equal to 35 seconds was obtained. The value of torque constant was approximately 3.8 ft.lbf/MPH ,

giving a gain constant of approximately 0.80.

A time constant of 35 seconds gave a very low value of acceleration on the hill of coefficient of power versus tip speed ratio characteristics. Besides the value of equivalent damping was approximately 0.41 ft.lbf.sec. to match prevailing initial values. To achieve appropriate value of initial acceleration for an initial value (non-zero initial value) problem, a time constant of 20 seconds was selected, which gave the wind rotor inertia of 8.2 ft.lbf.sec². A step change in wind speed does not bring a step change in torque developed by the wind rotor. The damping coefficient, B_{eq} , depends on operating point, but in the region of primary interest (on the top portion of the coefficient of power versus tip speed ratio characteristics) it was assumed to remain constant. The gain of the wind rotor in the operating range depends on the load. The simulation model is non-linear and therefore response curves are not exponential. The response of the rotor from zero rotor speed to a steady state speed is much slower than that from a steady state to a new steady state.

Based on available static characteristics the potential of the KSU Savonius wind machine for pumping water out of wells could be investigated analytically. More experimental data are needed for drawing the static characteristics more accurately. Further work could be carried out by considering more elaborate model for a synchronous machine. The electrical losses in the alternator are very high and therefore the efficiency of the automotive type alternator is very low. This calls for a better d.c. machine. A better mechanical power transmission system is required or a generator should be so selected that it requires a low speed ratio.

LIST OF REFERENCES

1. Bodek, A. and Simonds, M.H., "Performance Test Of A Savonius Rotor", Brace Research Institute, T.R. 10, McGill University, Canada, 1964.
2. Carver, C. and McPherson, R.B., "Experimental Investigation Of The Use Of A Savonius Rotor As A Power Generating Device", May 1974.
3. Cretzler, D.J., Gaul, R.D. and Snodgrass, J.M., "Some Dynamical Properties Of Savonius Rotor Current Meter", Marine Science Instrumentation, Volume 2, 1962.
4. Kimball, H. and Jeter, M., "The Determination Of The Relationship Between Applied Power To The Shaft Of The Automotive Type Alternator And Corresponding RPM, Armature Current, and Armature Voltage", Kansas State University, Seaton Hall, July 1975.
5. Kentfield, J.A.C., "A Modified Savonius Wind Turbine With Good Low Velocity-Ratio Torque Characteristics", Sherbrooke Conference Report, May 1974.
6. Kloeffer, R.G. and Sitz, E.L., "Electrical Energy From Winds", Engineering Experiment Station, Kansas State University, Bulletin Number 52, September 1946.
7. McPherson, R.B., "Design Development And Testing Of A Low Head, High Efficiency, Kinetic Energy Machine - An Alternative For The Future", September 1972.
8. Mercier, J.A., "Power Generating Characteristics Of Savonius Rotors", Davidson Laboratory, Stevens Institute Of Technology, Report 1181, 1966.
9. Newman, B.G., "Measurements On A Savonius Rotor With Variable Gap",

Sherbrooke University Symposium On Wind Energy, May 1974.

10. Savonius, S.J., "The S-Rotor And Its Applications", Mechanical Engineering, May 1931, 333-338.
11. Yates, F. and Fisher, R.A., "Statistical Tables", Oliver and Boyd, Edinburg, 1938.

APPENDIX I

COMPUTER PROGRAM FOR CALCULATION
OF LOAD (in ohms) ON THE OUTPUT
TERMINALS OF THE ALTERNATOR

\$JOB

```

10 READ (5,55) VW
   IF (VW.GT. 20.) GO TO 88
55 FORMAT (F10.0)
   PRINT,'THE WIND VELOCITY IN MPH IS ',VW
   TSR=.5
77 RG=.22
   GN=(16.*TSR*VW)/.2052
   RN=GN/16.
   ER=-.806+.01332*GN-.6E-07*GN*GN
   PFW=-2.88+.807E-02*GN+.2026E-04*GN*GN+.2629E-09*GN*GN*GN
   X2=TSR
   X3=VW
   X4=X2/X3
   X5=X4*X2
   X6=X2*X2*X2*X2*X3
   X7=(X6*X2)/(X3*X3)
   X8=X2*X3
   X9=1./((X3*X3*X3)
   A=-.0882718
   B2=3.61914063
   B3=.00334048
   B4=-20.24581909
   B5=-3.87563229
   B6=.0079651
   B7=-1.4449625
   B8=-.11441177
   B9=64.50268555
   EFF=A+B2*X2+B3*X3+B4*X4+B5*X5+B6*X6+B7*X7+B8*X8+B9*X9
   IF (EFF.LE. 0.09) GO TO 10
   TO=(.422876*EFF*VW*VW)/TSR
   PMECH=.2926*EFF*VW*VW*VW
   CURR=(PMECH-PFW)/EB
   VT=EB-CURR*RG
   RL=VT/CURR
   PEL=CURR*CURR*RG
   B=1.751-.5646*10.**(-4)*GN+.2527*10.**(-6)*GN*GN-.4241*10.**(-10)
   1*GN*GN*GN
   C=.7686-.4871*10.**(-3)*GN+.4172*10.**(-7)*GN*GN+.1398*10.
   1**(-10)*GN*GN*GN
   PELECT=C*CURR**B
   PRINT 11,TSR,RN,RL,EFF,CURR,VT,PEL,PELECT
11  FORMAT (/ ,8F16.6)
   TSR=TSR+.05
   IF (TSR-1.85) 77,10,10
88  PRINT,'NORMAL TERMINATION'
   STOP
   END

```

APPENDIX II

COMPUTER PROGRAM FOR AN INITIAL-VALUE
PROBLEM FOR NON-LINEAR LUMPED PARAMETER
SYSTEM USING RKG NUMERICAL TECHNIQUE

\$JOB

```

      DIMENSION Y(2),DY(2),Q(2)
      NEQ=2
      DO 10 I=1,NEQ
10    Q(I)=0.0
      H=.01

      Y(1)=8.8724
      Y(2)=11.03478
      T=0.00
      WRITE(6,55)
55    FORMAT(5X,'TIME',9X,'ROT SPEED',3X,'TERM CURR',5X,'ANG ACCLN',2X,
      *'RATE OF CHANGE',2X,'EB',9X,'VT',7X,'POUT',8X,'PELECT',6X,
      1'PMECH')
      WRITE(6,88)
88    FORMAT(/,56X,'OF CURRENT')
      WRITE(6,77)
77    FORMAT(/,5X,'SECS',8X,'RAD P SEC',6X,'AMPS',4X,'RAD P SECSEC',
      *1X,'AMP P SECSEC',5X,'VOLTS',7X,'VOLTS',9X,'WATTS',7X,'WATTS',
      17X,'WATTS')
      DO 20 L=1,50
      CALL RKG(NEQ,H,T,Y,DY,Q,PELECT,POUT,EB,VT)
      GN=960.*Y(2)/6.282
      PFW=-2.88+.807*10.**(-2)*GN+.2026*10.**(-4)*GN*GN+.2629*10.**
      1(-9)*GN*GN*GN
      PMECH=POUT+PELECT+PFW
      PRINT 11,T,Y(1),Y(2),DY(1),DY(2),EB,VT,POUT,PELECT,PMECH
11    FORMAT(10F13.7)
20    CONTINUE
      STOP
      END

```

```

      SUBROUTINE RKG(NEQ,H,X,Y,DY,Q,PELECT,POUT,EB,VT)
C    * * * * *
C    THE INDEPENDENT VARIABLE X IS INCREMENTED IN THIS PROGRAM
C    Y(I) AND DY(I) ARE THE DEPENDENT VARIABLE AND ITS DERIVATIVE
C    ALL THE Q(I) MUST BE INITIALLY SET TO ZERO IN THE MAIN PROGRAM
C    NEQ = NUMBER OF FIRST ORDER EQUATIONS
C    H = INTERVAL SIZE
C    A SUBROUTINE DERIV(NEQ,X,Y,DY) MUST BE PROVIDED
C    * * * * *
      DIMENSION A(2)
      DIMENSION Y(NEQ),DY(NEQ),Q(NEQ)
      A(1)=0.29289322
      A(2)=1.7071068
      H2=.5*H
      CALL DERIV(NEQ,X,Y,DY,PELECT,POUT,EB,VT)
      DO 13 I=1,NEQ
      B=H2*DY(I)-Q(I)
      Y(I)=Y(I)+B.
13    Q(I)=Q(I)+3.*B-H2*DY(I)
      X=X+H2
      DO 20 J=1,2
      CALL DERIV(NEQ,X,Y,DY,PELECT,POUT,EB,VT)
      DO 20 I=1,NEQ
      B=A(J)*(H*DY(I)-Q(I))
      Y(I)=Y(I)+B
20    Q(I)=Q(I)+3.*B-A(J)*H*DY(I)
      X=X+H2
      CALL DERIV(NEQ,X,Y,DY,PELECT,POUT,EB,VT)

```

```

00 26 I=1,NEQ
      B=0.166666667*(H*DY(I)-2.*Q(I))
Y(I)=Y(I)+B
26 Q(I)=Q(I)+3.*B-H2*DY(I)
RETURN
END

SUBROUTINE DERIV(NEQ,T,Y,DY,PELECT,POUT,EB,VT)
DIMENSION Y(2),DY(2)
REAL DJE,AKT,BKG,CLG
DJE=8.2
BE=.42
RG=.22
CLG=.022
VW=18.5
RN=9.5493*Y(1)
U=.20527*RN
TSR=U/VW
X2=TSR
X3=VW
X4=X2/X3
X5=X4*X2
X6=X2*X2*X2*X2*X3
X7=(X6*X2)/(X3*X3)
X8=X2*X3
X9=1./(X3*X3*X3)
A=-.0882718
B2=3.61914063
B3=.00334048
B4=-20.24581909
B5=-3.87563229
B6=.0079651
B7=-1.4449625
B8=-.11441177
B9=64.50268555
EFF=A+B2*X2+B3*X3+B4*X4+B5*X5+B6*X6+B7*X7+B8*X8+B9*X9
TO=(.422876*EFF*VW*VW)/TSR
GN=960.*Y(1)/6.282
A=.7686-.4871*10.**(-3)*GN+.4172*10.**(-7)*GN*GN+.1398*10.
1**(-10)*GN*GN*GN
B=1.751-.5646*10.**(-4)*GN+.2527*10.**(-6)*GN*GN-.4241*10.**(-10)
1*GN*GN*GN
PELECT=A*(Y(2))*B
EB=-.806+.01332*GN-.6*10.**(-7)*GN*GN
RL=1.333
VT=PL*Y(2)
POUT=VT*Y(2)
TR=(POUT+PELECT)*1.341*0.55/Y(1)

DY(1)=(TO-TR)-BE*Y(1))/DJE
DY(2)=(EB-VT-(RG*Y(2)))/CLG
RETURN
END

```

\$ENTRY

APPENDIX III

LINEARIZED TRANSFER FUNCTION FOR WIND ROTOR-ALTERNATOR SYSTEM

From equation 5-2:

$$T_{dev} = f(V_w, N_r) \quad \text{III-1}$$

And, for small changes about a steady state operating point:

$$\Delta T_{dev} = \frac{\partial T_{dev}}{\partial V_w} \Delta V_w + \frac{\partial T_{dev}}{\partial N_r} \Delta N_r \quad \text{III-2}$$

Also, equation 5-7 for small changes becomes:

$$J_{eq} \frac{d \Delta N_r}{dt} + B_{eq} \Delta N_r + \frac{60}{2\pi} (\Delta T_{ref} - \Delta T_{dev}) = 0 \quad \text{III-3}$$

Equation 5-9 can be written as follows:

$$T_{ref} = f(P_{out}, P_{elect}, N_r) \quad \text{III-4}$$

Then, since $P_{out} = f(V_L, I_L)$, $P_{elect} = f(N_r, I_L)$ and $V_L = I_L R_L$, equation III-4 can be rewritten as follows for small changes:

$$\Delta T_{ref} = \frac{\partial T_{ref}}{\partial N_r} \Delta N_r + \left(\frac{\partial T_{ref}}{\partial V_L} R_L + \frac{\partial T_{ref}}{\partial I_L} \right) \Delta I_L \quad \text{III-5}$$

Now since $E_b = f(N_r)$, see equation 5-10, equation 5-8 can be written as follows for small changes:

$$L_a \frac{d \Delta I_L}{dt} + (R_a + R_L) \Delta I_L - \frac{\partial E_b}{\partial N_r} \Delta N_r = 0 \quad \text{III-6}$$

Taking the Laplace Transform and solving for $\Delta I_L(s)$ yields:

$$\Delta I_L(s) = \frac{K_a}{(T_a s + 1)} \Delta N_r(s) \quad \text{III-7}$$

where:

$$K_a = \frac{\frac{\partial E_b}{\partial N_r}}{R_a + R_L}$$

Substituting equation III-7 into equation III-5 yields:

$$\Delta T_{ref} = \frac{\partial T_{ref}}{\partial N_r} \Delta N_r + \left(\frac{\partial T_{ref}}{\partial V_L} R_L + \frac{\partial T_{ref}}{\partial I_L} \right) \frac{K_a \Delta N_r(s)}{(T_a s + 1)} \quad \text{III-8}$$

Now taking the Laplace Transform of all equations, then substituting equations III-2 and III-8 into III-3, and finally solving for $\frac{\Delta N_r(s)}{\Delta V_w(s)}$ yields:

$$\frac{\Delta N_r(s)}{\Delta V_w(s)} = \frac{K_g (T_a s + 1)}{(J s^2 + B s + K)} \quad \text{III-9}$$

Factoring the denominator gives:

$$\frac{\Delta N_r(s)}{\Delta V_w(s)} = \frac{T T' K_g (T_a s + 1)}{(T s + 1) (T' s + 1)} \quad \text{III-10}$$

where,

$$\frac{1}{T} = \frac{-B - \sqrt{B^2 - 4JK}}{2J} \quad \text{and} \quad \frac{1}{T'} = \frac{-B + \sqrt{B^2 - 4JK}}{2J}$$

$$K_g = \frac{60}{2\pi} \frac{\partial T_{dev}}{\partial V_w}$$

$$J = J_{eq} T_a$$

$$B = J_{eq} + B_{eq} T_a + \frac{60}{2\pi} T_a \left(\frac{\partial T_{ref}}{\partial N_r} - \frac{\partial T_{dev}}{\partial N_r} \right)$$

$$K = C_L K_a + B_{eq} + \frac{60}{2\pi} \left(\frac{\partial T_{ref}}{\partial N_r} - \frac{\partial T_{dev}}{\partial N_r} \right)$$

$$C_L = \frac{60}{2\pi} \left(\frac{\partial T_{ref}}{\partial V_L} R_L + \frac{\partial T_{ref}}{\partial I_L} \right)$$

$$K_r = K_g T T'$$

In the range of primary interest it appears that the denominator has real poles and that one of the real poles produces a pole-zero cancellation effect. Therefore, equation III-10 can be rewritten as follows:

$$\frac{\Delta N_r(s)}{\Delta V_w(s)} = \frac{K_r}{(T s + 1)} + \frac{N_r(0)}{\Delta V_w(s)} \quad \text{III-11}$$

ACKNOWLEDGEMENTS

The author wishes to express his appreciation to his major advisor, Dr. R.O. Turnquist of the Mechanical Engineering Department, Dr. J. Garth Thompson of the Mechanical Engineering Department and Dr. F.W. Harris of the Electrical Engineering Department.

THE STATIC AND DYNAMIC PERFORMANCE
CHARACTERISTICS OF THE KSU SAVONIUS WIND ROTOR

by

SHAILESH HARIPRASAD PATEL

B.E., The Maharaja Sayajirao University Of Baroda, India, 1973

AN ABSTRACT OF MASTER'S THESIS

submitted in partial fulfillment of the
requirements for the degree

MASTER OF SCIENCE

Department of Mechanical Engineering

Kansas State University

Manhattan, Kansas

1977

ABSTRACT

A vertical axis rotary type wind energy collecting system was designed, built and field-tested by some faculty and students of Mechanical and Electrical Engineering. This rotor is known as Savonius rotor. The data were taken during July, 1975. The wind rotor was loaded by an automobile alternator. The static performance characteristics were established by making use of the collected data. Mathematical models were then obtained for these static characteristics by using statistical computer programs for regression. To obtain the dynamic performance characteristics, a propagation problem for non-linear lumped parameter system (wind rotor-alternator) was then discussed. The torque developed by the wind rotor and the torque reflected due to the load introduced nonlinearity in the differential equation representing the wind rotor. The static characteristics helped in determining the value of load resistance on the alternator for constant load operation without much impairing the coefficient of power, maximum coefficient of power operation and constant speed operation. The static torque-speed characteristics gave the torque equation for the linear range. It also gave transfer function for the wind rotor for zero initial condition. The transfer function for non-zero initial conditions is derived with the help of the time-domain analysis and the torque-speed characteristics.